

**MEASUREMENT OF DENSITY, ISOTHERMAL
COMPRESSIBILITY, HEAT CAPACITY RATIO FOR
ESTIMATING SONIC VELOCITY OF RESERVOIR FLUIDS.**

By

Hassan A. Alkandari

1997

**ARTHUR LAKES LIBRARY
COLORADO SCHOOL OF MINES
GOLDEN, CO 80401**

ProQuest Number: 10794308

All rights reserved

INFORMATION TO ALL USERS

The quality of this reproduction is dependent upon the quality of the copy submitted.

In the unlikely event that the author did not send a complete manuscript and there are missing pages, these will be noted. Also, if material had to be removed, a note will indicate the deletion.



ProQuest 10794308

Published by ProQuest LLC (2018). Copyright of the Dissertation is held by the Author.

All rights reserved.

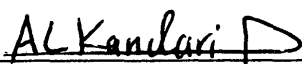
This work is protected against unauthorized copying under Title 17, United States Code
Microform Edition © ProQuest LLC.


ProQuest LLC.
789 East Eisenhower Parkway
P.O. Box 1346
Ann Arbor, MI 48106 – 1346

A thesis submitted to the faculty and the board of Trustees of the Colorado School of Mines in partial fulfillment of the requirements for the degree of Master of Science in Petroleum Engineering.

Golden, Colorado

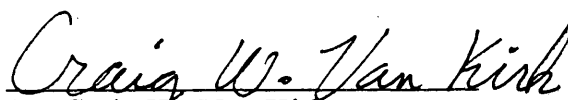
Date: Sep 2nd, '97

Signed: 
Hassan Ahmad Alkandari

Approved: 
Dr. Richard L. Christiansen
Thesis Advisor

Golden, Colorado

Date: September 2, 1997


Dr. Craig W. Van Kirk
Head, Department of
Petroleum Engineering.

ABSTRACT

The long-term objective of this work is to improve correlations for estimating seismic velocities of fluids in exploration basins and in developing reservoirs. These correlations must be simple enough to allow convenient use by workers with a wide variety of technical background. In order to estimate sonic velocity of these fluids, an accurate measurement of fluid density, isothermal compressibility, and heat capacity ratio is required.

In this work, an apparatus was assembled for measuring the isothermal compressibility of a single phase fluid. During testing of the apparatus, it was noticed that the transient pressure data from a compressibility measurement give an estimate of the heat capacity ratio. Until now, heat capacity ratios for crude oils are largely, if not entirely, unavailable in the oil industry literature.

In this project, the isothermal compressibility and the heat capacity ratios were measured for decane, Burly oil sample, de-ionized water, and n-pentane, and compared to the available literature values. Satisfactory comparisons were obtained and noted. Sonic velocities were calculated from the measured values of isothermal compressibility, heat capacity ratio, and estimates of densities, and

compared with the readings obtained by Dr. Batzle's group in the Geophysics Department.

From the excellent results for the four different fluid samples, it was concluded that the new apparatus yields sufficiently accurate values of isothermal compressibility and heat capacity ratio for single phase fluids.

TABLE OF CONTENTS

	Page
ABSTRACT.....	iii
TABLE OF CONTENTS.....	v
LIST OF FIGURES.....	vii
LIST OF TABLES.....	x
ACKNOWLEDGMENTS.....	xi
Chapter 1: INTRODUCTION.....	1
Chapter 2: LITERATURE REVIEW.....	7
2.1 Wave Velocity.....	7
2.2 Compressibility.....	15
2.3 Heat Capacity Ratio.....	19
Chapter 3: EXPERIMENTAL PROCEDURES.....	25
3.1 Experimental Apparatus.....	25
3.2 Experimental Procedure.....	31
3.3 Dead Volume Error in Compressibility Measurement.....	31
3.4 Time for Thermal Equilibration.....	34

	Page
Chapter 4: EXPERIMENTAL RESULTS.....	36
4.1 Decane Sample.....	37
4.2 Burly Oil Sample.....	50
4.3 De-ionized water sample.....	55
4.4 n-Pentane Sample.....	70
Chapter 5: CONCLUSIONS AND RECOMMENDATIONS.....	82
5.1 Conclusions.....	82
5.2 Recommendations.....	84
REFERENCES.....	87
APPENDICES.....	90

LIST OF FIGURES

	Page
Figure 2.1: Typical Shape of the Coefficient of isothermal compressibility of Oils as a function of pressure at a constant reservoir temperature.....	17
Figure 3.1: Schematic of Apparatus for Measuring Fluids Compressibility...	26
Figure 3.2: Pressure vs. Time for a Decane sample.....	29
Figure 3.3: The effect of poor temperature control for Pentane sample.....	30
Figure 4.1: Pressure history for Decane sample at 72°F (Run 1).....	41
Figure 4.2: Pressure history for Decane sample at 72°F (Run 2).....	42
Figure 4.3: Pressure history for Decane sample at 104°F (Run 1).....	43
Figure 4.4: Pressure history for Decane sample at 104°F (Run 2).....	44
Figure 4.5: Pressure history for Decane sample at 140°F (Run 1).....	45
Figure 4.6: Pressure history for Decane sample at 140°F (Run 2).....	46
Figure 4.7: Pressure history for Decane sample at 176°F (Run 1).....	47
Figure 4.8: Pressure history for Decane sample at 176°F (Run 2).....	48
Figure 4.9: Sonic Velocity values for decane.....	49
Figure 4.10: Pressure history for Burly Oil sample at 104°F (Run 1).....	51

	Page
Figure 4.11: Pressure history for Burly Oil sample at 104°F (Run 2).....	52
Figure 4.12: Pressure history for Burly Oil sample at 104°F (Run 3).....	53
Figure 4.13: Sonic Velocity values for Burly Oil.....	54
Figure 4.14: Pressure history for de-ionized water sample at 71°F (Run 1)....	59
Figure 4.15: Pressure history for de-ionized water sample at 71°F (Run 2)....	60
Figure 4.16: Pressure history for de-ionized water sample at 100°F (Run 1)...	61
Figure 4.17: Pressure history for de-ionized water sample at 100°F (Run 2)...	62
Figure 4.18: Pressure history for de-ionized water sample at 150°F (Run 1)...	63
Figure 4.19: Pressure history for de-ionized water sample at 150°F (Run 2)...	64
Figure 4.20: Pressure history for de-ionized water sample at 200°F (Run 1)...	65
Figure 4.21: Pressure history for de-ionized water sample at 200°F (Run 2)...	66
Figure 4.22: Water heat capacity ratio as a function of pressure.....	67
Figure 4.23: Water heat capacity ratio as a function of temperature.....	68
Figure 4.24: Sonic Velocity values for n-Pentane.....	69
Figure 4.25: Pressure history for n-Pentane sample at 68°F.....	74
Figure 4.26: Pressure history for n-Pentane sample at 104°F (Run 1).....	75
Figure 4.27: Pressure history for n-Pentane sample at 104°F (Run 2).....	76

	Page
Figure 4.28: Pressure history for n-Pentane sample at 140°F (Run 1).....	77
Figure 4.29: Pressure history for n-Pentane sample at 140°F (Run 2).....	78
Figure 4.30: Pressure history for n-Pentane sample at 176°F (Run 1).....	79
Figure 4.31: Pressure history for n-Pentane sample at 176°F (Run 2).....	80
Figure 4.32: Sonic Velocity values for n-Pentane.....	81

LIST OF TABLES

	Page
Table 4.1 Measured and literature density values for n-decane, Burly oil, de-ionized water, and n-pentane.....	37
Table 4.2 Measured and literature obtained isothermal compressibilities and heat capacity ratios for n-decane.....	39
Table 4.3 Calculated sonic velocity of n-decane for both literature obtained and laboratory measured data.....	40
Table 4.4 Measured isothermal compressibilities, heat capacity ratios, and sonic velocities for Burly oil sample at 104 °F.....	50
Table 4.5 Measured and literature obtained isothermal compressibilities and heat capacity ratios for de-Ionized water.....	57
Table 4.6 Calculated sonic velocity of de-ionized water for both literature obtained and laboratory measured data.....	58
Table 4.7 Measured and literature obtained isothermal compressibilities and heat capacity ratios for n-pentane.....	72
Table 4.8 Calculated sonic velocity of n-pentane for both literature obtained and laboratory measured data.....	73

ACKNOWLEDGMENT

I would like to express my deepest gratitude and sincere appreciation to my thesis advisor, Professor Richard Christiansen, for his constant support, continued encouragement, and great assistance in this research.

Thanks and appreciation are also extended to committee members Professor Michael Batzle and Professor Robert Thompson. Professor Batzle provided valuable sonic velocity data for comparisons to estimates with my data.

I also wish to thank Abdulrahman Al- Kraishi for his suggestions and help to complete this work.

Financial support for purchase of supplies for modifying the apparatus was provided by the fluids consortium managed by Professor Batzle. The members of the consortium are Amerada Hess, Amoco, Arco, BHP, BP, Chevron, Conoco, Exxon, Jnoc, Marathon, Mobil, Norsk Hydro, Phillips, PGS, Saga, Saudi Aramco, Shell, Statoil, Texaco, Total, and Unocal.

The temperature bath and accessories were purchased with funds provided by Shell Foundation.

CHAPTER ONE

INTRODUCTION

Seismic techniques for identifying hydrocarbon traps rely on the slight sensitivity of seismic properties of rocks (e.g., velocity) to fluid content. The nature of fluids in the pore spaces of the rock affect the seismic properties in a subtle way. As a result, the seismic data includes some information about fluids present in formations. Recovering fluid saturation information from the seismic data presents significant challenges to the oil and gas industry.

To recover fluid saturations from seismic data, accurate knowledge of the seismic properties of the fluids and the effect of the fluids on the seismic properties of the rock is needed. Little effort has been made toward using accurate fluid properties in seismic exploration. The purpose of this work is to improve correlations for estimating the relevant seismic properties of fluids in exploration basins and in developing reservoirs. These correlations must be simple enough to allow convenient use by workers with a wide variety of technical backgrounds. In order to estimate the sonic velocity of the tested fluids, a precise measurement of fluid density, isothermal compressibility, and heat capacity ratio is required.

Therefore an apparatus was assembled for measuring the isothermal compressibility of a single phase fluid. During the testing of our apparatus, it was noticed that instantaneously after decreasing the cell volume, the pressure rose rapidly and then slowly decreased to a stable reading. The ratio of the instantaneous pressure rise to the stabilized pressure decline can be used to estimate the heat capacity ratio of the sample being tested. So, in addition to isothermal compressibility, the apparatus have perfectly yielded heat capacity ratios, which can be calculated as follows,

$$\frac{c_p}{c_v} = \frac{\Delta p_{inst.}}{\Delta p_{stab.}} \quad (1.1)$$

where,

c_p = heat capacity at constant pressure,

c_v = heat capacity at constant volume,

$\Delta p_{inst.}$ = | Peak Pressure - Initial Pressure |,

$\Delta p_{Stab.}$ = | Stabilized Pressure - Initial Pressure |

In this project, the isothermal compressibility and the heat capacity ratios will be measured for decane, Burly oil, de-ionized water, and n-pentane, and then compared to the available literature values. Then, sonic velocities will be calculated from the measured values of isothermal compressibility, heat capacity

ratio, and estimates of densities, and compared with the readings computed by Dr. Batzle in the Geophysics Department.

In the following chapter, fluid properties of concern in this research, such as wave velocity, isothermal and adiabatic compressibility, and heat capacity ratio will be introduced and discussed. Seismic waves in solids have compressional and shear components. The compressional (or longitudinal) component of the seismic wave is the subject of this thesis. Isothermal and adiabatic compressibility can be defined as a fractional change in volume due to change in pressure, which can be referred to as,

$$c = -\left(\frac{1}{v}\right)\left(\frac{\Delta v}{\Delta p}\right)_T \quad (1.2)$$

where,

c = compressibility, psi^{-1}

v = volume of the vessel, cm^3

Δv = change in volume, cm^3

Δp = change of pressure, psi .

If the volume changes at a constant temperature, the compressibility is known as isothermal compressibility, and if there was no heat transfer between the system and its surroundings, then it is referred to as an adiabatic compressibility. And

finally, heat capacity ratio will be presented in this chapter. Heat capacity ratio is the key function to switch back and forth between adiabatic and isothermal compressibility, which can simply be presented as,

$$c_{\text{adiabatic}} = c_{\text{isothermal}} \frac{c_p}{c_v} \quad (1.3)$$

where,

$$c_p = \left(\frac{\partial h}{\partial T} \right)_p = \text{heat capacity at constant pressure,}$$

$$\left(\frac{\partial h}{\partial T} \right)_p = \text{change in enthalpy with respect to temperature at constant pressure,}$$

$$\left(\frac{\partial u}{\partial T} \right)_v = \text{change in internal energy with respect to temperature at constant volume,}$$

$$c_v = \left(\frac{\partial u}{\partial T} \right)_v = \text{heat capacity at constant volume}$$

Therefore, the adiabatic compressibility equals the isothermal compressibility when the heat capacity equals unity.

In chapter three, the experimental apparatus, design, and the experimental procedure conducted to determine the isothermal compressibility and heat capacity

ratios are discussed and explained. An apparatus was assembled to measure isothermal compressibility, which contains a high pressure positive displacement pump, a transfer vessel, tubing, valves, and pressure transducer all placed inside a temperature controlled air bath. While designing the apparatus, the following PVT factors were of a concern, pressure, volume, and temperature for both inside and outside the controlled temperature air bath. Stabilization time was considered in order to predict the length of the experiment and the time needed to get predictable results. The apparatus was designed to be a user friendly as much as possible and to have an easy operational procedure.

In chapter four, both the laboratory measured and the collected data are compared and analyzed for all four samples, (decane, Burly oil, de-ionized water, and n-pentane) respectively. The data measurement of the samples were first to measure the density, isothermal compressibility, and heat capacity ratio for the four known samples, and then use the measured data to calculate the sonic velocity. The figures in this chapter confirm the time of stabilization and the accuracy of the experiments conducted.

In chapter five, conclusions are discussed to present the improved correlations between literature and measured data of density, isothermal

compressibility, and heat capacity ratios to better estimate the sonic velocity. Also recommendations are being made for future studies to follow this thesis.

References are being presented after chapter five for additional information. And finally appendices are included to show sample calculations, data measured and data obtained from literature, and correlations between them to estimate sonic velocity.

CHAPTER TWO

LITERATURE REVIEW

In this chapter, fluid properties of concern in this research, such as wave velocity, isothermal and adiabatic compressibility, and heat capacity ratio, will be discussed.

2.1 Wave Velocity from Thermodynamics

Seismic waves are groups of compressional and shear strain energy that propagate outward from a seismic source. The compressional (or longitudinal) component of the seismic wave is the subject of this thesis. The compressional wave velocity (v_p) is called “longitudinal” because the compressional component is parallel to the direction of propagation. Kearey (1991) states that a good example of compressional waves is sound which is a disturbance of the molecules of air with a frequency which can be detected by ear. The velocity of a compressional wave through a homogenous medium(single phase) liquid is

$$v_p = \sqrt{\left(\frac{\partial p}{\partial \rho}\right)_s} \quad (2.1)$$

where,

v_p = compressional wave velocity,

p = pressure, and

ρ = density.

Equation 2.1 is obtained from a momentum balance of a compressional wave passing through a differential volume element of cross-sectional area A . According to Fowler (1958) the force difference from inlet to outlet is equal to the change in momentum is expressed as follows,

$$pA - (p + dp)A = \rho v_p^2 A - (\rho + d\rho)v_p^2 A \quad (2.2)$$

where,

A = cross sectional area,

dp = change in pressure,

v_p = sonic velocity, and

$d\rho$ = change in density.

By expanding Eq. 2.2, the following expression is obtained:

$$pA - pA - Adp = \rho v_p^2 A - \rho v_p^2 A - v_p^2 Ad\rho \quad (2.3)$$

Simplifying Equation 2.3 by canceling terms, yields,

$$dp = d\rho v_p^2 \quad (2.4)$$

or,

$$v_p = \sqrt{\frac{dp}{d\rho}} \quad (2.5)$$

The derivative in Eq. 2.5 is normally taken to be at constant entropy, because the compression of the fluid occurs quickly without opportunity for heat transfer, and because the compression is small. So, the compression is considered to be reversible and adiabatic, or at constant entropy.

An alternative expression for wave velocity, Eq. 2.1, can be obtained by using the specific volume which is the inverse of the density:

$$v = \frac{1}{\rho} \quad (2.6)$$

where,

$$\rho = \frac{m}{v},$$

$m = \text{mass}$

Then,

$$d\rho = -\frac{dv}{v^2} \quad (2.7)$$

and Eq. 2.1 can be written as,

$$v_p = v \sqrt{-\left(\frac{\partial p}{\partial v}\right)_s} \quad (2.8)$$

According to Andsager (1967) acoustic velocities can be calculated from relationship which involves atmospheric heat capacity ratios rather than heat capacity ratios which are a function of pressure. As has been pointed out by Thomas (1968) this approximate relationship provides a good working equation for calculating acoustic velocities at low pressure ranges, and should not be used at high pressure range.

Equation 2.8 can be modified with the following expression from the thermodynamic literature using Hougen *et al.*(1974) relationship to contain the heat capacity ratio (derived below):

$$\left(\frac{\partial p}{\partial v}\right)_s = \frac{c_p}{c_v} \left(\frac{\partial p}{\partial v}\right)_T \quad (2.9)$$

where,

c_p = heat capacity at constant pressure,

c_v = heat capacity at constant volume,

s = entropy, and,

T = temperature.

Using Eq. 2.9, the expression for v_p in Eq. 2.8 becomes

$$v_p = v \sqrt{-\frac{c_p}{c_v} \left(\frac{\partial p}{\partial v} \right)_T} \quad (2.10)$$

Isothermal compressibility of a fluid is defined as,

$$c = -\left(\frac{1}{v} \right) \left(\frac{\partial v}{\partial p} \right)_T \quad (2.11)$$

where,

c = isothermal compressibility, psi^{-1}

v = volume, cm^3

p = pressure, psi .

Combining the definition of Eq. 2.11 with Eq. 2.10, then

$$v_p = \sqrt{-\frac{c_p v}{c_v c}} \quad (2.12)$$

Equation 2.9, which is essential for introducing heat capacity ratios to the velocity expression, may be derived from basic thermodynamic relations, as described by Hougen *et al.*(1974). First, heat capacities are defined as follows,

$$c_p = \left(\frac{\partial h}{\partial T} \right)_p \quad (2.13)$$

$$c_v = \left(\frac{\partial u}{\partial T} \right)_v \quad (2.14)$$

From the fundamental relations for enthalpy, h , and internal energy, u ,

$$dh = Tds + vdp \quad (2.15)$$

$$du = Tds + pdv \quad (2.16)$$

then,

$$\left(\frac{\partial h}{\partial T}\right)_P = T \left(\frac{\partial s}{\partial T}\right)_P \quad (2.17)$$

$$\left(\frac{\partial u}{\partial T}\right)_V = T \left(\frac{\partial s}{\partial T}\right)_V \quad (2.18)$$

Using the definitions of heat capacities, then Eqs. 2.17 and 2.18 become

$$c_p = T \left(\frac{\partial s}{\partial T}\right)_P \quad (2.19)$$

$$c_v = T \left(\frac{\partial s}{\partial T}\right)_V \quad (2.20)$$

The ratio of Eqs. 2.19 and 2.20 gives an expression for the heat capacity ratio:

$$\frac{c_p}{c_v} = \frac{T \left(\frac{\partial s}{\partial T}\right)_P}{T \left(\frac{\partial s}{\partial T}\right)_V} \quad (2.21)$$

Further modification of Eq. 2.21 is possible by recognizing that entropy, s , is a state function of pressure and temperature. Then,

$$ds = \left(\frac{\partial s}{\partial p}\right)_T dp + \left(\frac{\partial s}{\partial T}\right)_P dT \quad (2.22)$$

If entropy is constant, then Eq. 2.22 becomes,

$$0 = \left(\frac{\partial s}{\partial p} \right)_T \left(\frac{\partial p}{\partial T} \right)_s + \left(\frac{\partial s}{\partial T} \right)_p \quad (2.23)$$

or,

$$\left(\frac{\partial s}{\partial T} \right)_p = - \left(\frac{\partial s}{\partial p} \right)_T \left(\frac{\partial p}{\partial T} \right)_s \quad (2.24)$$

Alternatively, if entropy is considered as a state function of volume and temperature, then,

$$ds = \left(\frac{\partial s}{\partial v} \right)_T dv + \left(\frac{\partial s}{\partial T} \right)_v dT \quad (2.25)$$

Following the pattern for deriving Eq. 2.24, then

$$\left(\frac{\partial s}{\partial T} \right)_v = - \left(\frac{\partial s}{\partial v} \right)_T \left(\frac{\partial v}{\partial T} \right)_s \quad (2.26)$$

Now, the expressions of Eqs. 2.24 and 2.26 can be used to modify the expression for heat capacity ratio in Eq. 2.21:

$$\frac{c_p}{c_v} = \frac{T \left(\frac{\partial s}{\partial T} \right)_p}{T \left(\frac{\partial s}{\partial T} \right)_v} = \frac{\left(\frac{\partial s}{\partial p} \right)_T \left(\frac{\partial p}{\partial T} \right)_s}{\left(\frac{\partial s}{\partial v} \right)_T \left(\frac{\partial v}{\partial T} \right)_s} \quad (2.27)$$

Using the chain rule for the two ratios of derivatives on the right side of Eq. 2.27, then

$$\frac{c_p}{c_v} = \left(\frac{\partial v}{\partial p} \right)_T \left(\frac{\partial p}{\partial v} \right)_s \quad (2.28)$$

And finally,

$$\left(\frac{\partial p}{\partial v} \right)_s = \frac{c_p}{c_v} \left(\frac{\partial p}{\partial v} \right)_T \quad (2.29)$$

The discussion above showed the relationship of wave velocity to thermodynamic properties. If sufficient thermodynamic data is available, then wave velocity could be estimated with Eq. 2.12 for example. However, the data needed for Eq. 2.12 are normally not available. As a result, some researchers have developed correlations for wave velocity in crude oils using convenient oil-field parameters. The acoustic velocity for crude oil can be estimated according to Wang *et al.* (1990) as

$$v_p = 215 + 50700 (77.1 + \text{API})^{-\frac{1}{2}} - 6.72T + 0.1096 p - \left(0.00166 \text{API}^{\frac{1}{2}} \right) p - \left(1.44 \cdot 10^{-4} - 5.18 \cdot 10^{-5} \text{API}^{\frac{1}{2}} \right) T p \quad (2.30)$$

where,

v_p = acoustic velocity, m/s,

API = Oil Gravity, °API,

T = temperature, °C,

p = pressure, bars.

2.2 Compressibility

Compressibility, either isothermal or adiabatic, is defined as the fractional change in volume due to a change in pressure. If the volume changes at a constant temperature, the compressibility is defined as isothermal compressibility, as defined in Eq. 2.11.

The most familiar compressibility in the petroleum industry is the isothermal compressibility. Isothermal compressibility of a fluid, above its bubble-point pressure, is defined as in Eq. 2.11. Figure 2.1 is a general trend plot of compressibility vs. pressure. As can be seen compressibility decreases with increasing pressure.

When the pressure is below the bubble-point pressure, isothermal compressibility of the fluids is defined by McCain (1990) as,

$$c_o = -\frac{1}{B_o} \left[\left(\frac{\partial B_o}{\partial P} \right)_T - B_g \left(\frac{\partial R_s}{\partial P} \right)_T \right] \quad (2.31)$$

where,

B_o = oil formation volume factor, RB/STB,

B_g = gas formation volume factor, RB/STB,

R_s = solution gas-oil ratio, SCF/STB.

Macias and Ramey (1986) demonstrated computation of isothermal compressibilities for multiphase, multicomponent systems. They observed that the compressibility of a gas-liquid system can exceed the compressibility of the gas phase alone. The application of their work was to well testing. They did not consider the application of their findings to seismic analysis.

Adiabatic compressibility is the fractional change in volume that accompanies a pressure change in a reversible adiabatic process:

$$c_{\text{adiabatic}} = -\left(\frac{1}{v}\right)\left(\frac{\partial v}{\partial p}\right)_s \quad (2.32)$$

An adiabatic process is one for which there is no heat transfer between the system and its surroundings. As suggested in the previous section and also by Castanga *et al.* (1993) adiabatic and isothermal compressibilities are related by

$$c_{\text{adiabatic}} = c_{\text{isothermal}} \frac{c_p}{c_v} \quad (2.33)$$

The adiabatic compressibility equals the isothermal compressibility when the heat capacity ratio equals unity, as is evident by examination of Eq. 2.29.

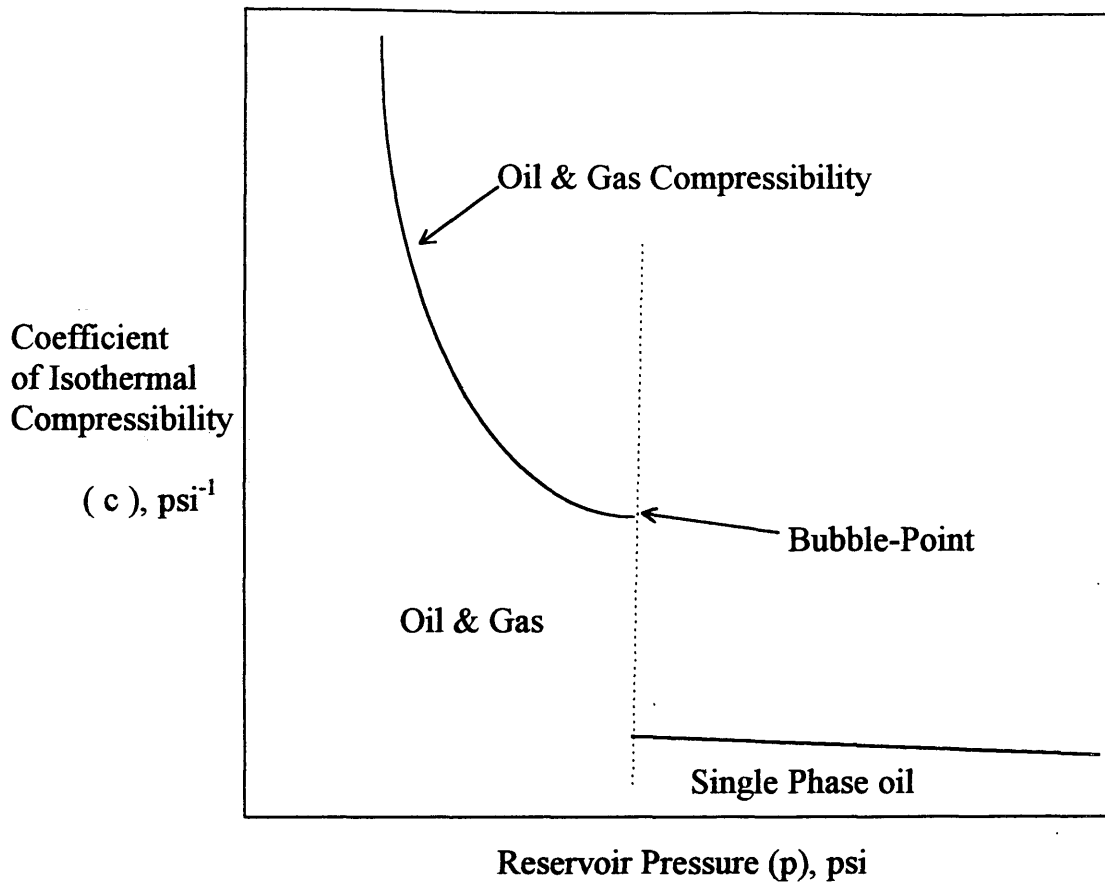


Figure 2.1 Typical Shape of the coefficient of isothermal compressibility of oil as a function of pressure at a constant reservoir temperature.

Adiabatic compressibility should be used in estimating acoustic wave velocity through a homogeneous phase rather than isothermal compressibility. While adiabatic compressibility is appropriate for estimating acoustic wave velocities of homogenous (single-phase) material, it may not be appropriate for estimating acoustic wave velocities in heterogeneous (multi-phase) such as a porous medium saturated with gas and liquids. Sonic velocities calculated by Keiffer (1977) for water-air and water-steam systems were smaller than for gas systems, presumably because of the extra compressibility of these two-phase systems.

Isothermal compressibilities for n-decane and n-pentane have been measured and reported by Vargaftik (1983). The data collected from the literature for n-decane, and n-pentane have been converted to field units as shown in Appendices A.1, and A.2. The isothermal compressibility for water has been reported by McCain, (1990) in graphical form(his Fig. 16.12) and as the following equation which is only applicable for temperatures above 200°F and high pressures:

$$c_w = \frac{1}{(A_1p + A_2S + A_3T + A_4)} \quad (2.34)$$

where,

c_w = water isothermal compressibility, psi^{-1} ,

p = pressure, psi ,

T = temperature, $^{\circ}\text{F}$,

A_1 = 7.033,

A_2 = 0.5415,

A_3 = -537.0,

A_4 = 403,300, and,

S = salinity, mg/l .

2.3 Heat Capacity and Heat Capacity Ratio

Heat capacity can be defined as the path-dependent heat needed to raise the temperature of a given mass of any material by one degree according to Smith (1975) as:

$$c \equiv \left(\frac{dq}{dT} \right)_{\text{path}} \quad (2.35)$$

where,

dq = quantity of heat per unit mass,

dT = the change in temperature.

The paths of most interest are constant volume and constant pressure paths.

For a constant volume path,

$$du = dq_v \quad (2.36)$$

So, the heat capacity at constant volume

$$c_v = \left(\frac{\partial u}{\partial T} \right)_v \quad (2.37)$$

For a constant pressure path,

$$dh = dq_p \quad (2.38)$$

So, the heat capacity at constant pressure is

$$c_p = \left(\frac{\partial h}{\partial T} \right)_p \quad (2.39)$$

Experimentally, Kyle (1992) states that the constant-pressure heat capacity is determined from enthalpy change measurement.

According to Wang *et al.* (1988) the acoustic velocity in a fluid can be related to thermal expansion and specific heats of fluids by using the following thermodynamic relation:

$$v_p^2 = \frac{c_p (\gamma - 1)}{T \alpha^2} \quad (2.40)$$

where,

$$\alpha = \frac{1}{v} \left(\frac{\partial v}{\partial T} \right)_p, \text{ Coefficient of thermal expansion,}$$

c_p = heat capacity at constant pressure,

T = absolute temperature,

$$\gamma = \frac{c_p}{c_v}, \text{ and,}$$

c_v = heat capacity at constant volume.

The thermal expansion and specific heats are generally related to the density of the fluid or its API gravity.

Heat capacity data in the literature are quite limited. For pure fluids of interest in this research, few constant-pressure heat capacities were found. Vargaftik (1983) gives tables of c_p for liquid n-decane and n-pentane at a variety of temperatures and pressures. For water, c_p data were obtained from Helgeson and Kirkham (1974). No constant volume heat capacities were found. And, no heat capacity ratios were found for fluids of interest. But, using relations from thermodynamics, heat capacity ratios can be calculated if constant-pressure heat capacities are combined with coefficients of thermal expansion and compressibilities for temperatures and pressures of interest. The procedure for this calculation is derived below.

From Walas(1985), the following expression for the difference between c_p and c_v is obtained:

$$c_p - c_v = -T \frac{\left(\frac{\partial v}{\partial T}\right)_p^2}{\left(\frac{\partial v}{\partial p}\right)_T} \quad (2.41)$$

The partial derivatives on the right of Eq. 2.41 can be modified using the definitions of the coefficients of compressibility and thermal expansion to obtain

$$c_p - c_v = T \frac{\alpha^2 T v}{c v} = \frac{\alpha^2 T v}{c} \quad (2.42)$$

with

$$c = -\frac{1}{v} \left(\frac{\partial v}{\partial P}\right)_T \quad (2.43)$$

and

$$\alpha = \frac{1}{v} \left(\frac{\partial v}{\partial T}\right)_p \quad (2.44)$$

Dividing Eq. 2.42 by c_p , then

$$1 - \frac{c_v}{c_p} = \frac{\alpha^2 T v}{c c_p} \quad (2.45)$$

With some further rearranging, the desired expression for the heat capacity ratio is obtained:

$$\frac{c_p}{c_v} = \left[1 - \frac{\alpha^2 T v}{c c_p} \right]^{-1} \quad (2.46)$$

Application of this expression will be demonstrated below for n-decane at 40°C and 40 atm. From Vargaftik(1983),

$$c = 1490 \cdot 10^{-7} \frac{\text{cm}^2}{\text{kg}}$$

$$c_p = 2.261 \frac{\text{kJ}}{\text{kg}^\circ\text{C}}$$

$$\alpha = 1029 \cdot 10^{-6} \frac{1}{^\circ\text{C}}$$

$$v = 1.384 \cdot 10^{-3} \frac{\text{m}^3}{\text{kg}}$$

Except for c , the units provided by Vargaftik are SI. The units of c will be converted first to SI, then the calculation will proceed in SI.

$$c = 1490 \cdot 10^{-7} \frac{1}{\frac{\text{kgf}}{\text{cm}^2}} \frac{1 \text{ kgf} / \text{cm}^2}{9.807 \cdot 10^4 \text{ N} / \text{m}^2} = 1.519 \cdot 10^{-9} \frac{\text{m}^2}{\text{N}}$$

Substituting the appropriate values in Eq. 2.45, then

$$\frac{\alpha^2 T v}{c c_p} = \frac{\left(1.029 \cdot 10^{-3} \frac{1}{\text{K}}\right)^2 (273 + 40)^\circ \text{K} \left(1.384 \cdot 10^{-3} \frac{\text{m}^3}{\text{kg}}\right)}{\left(1.519 \cdot 10^{-9} \frac{\text{m}^2}{\text{N}}\right) \left(2.261 \cdot 10^3 \frac{\text{J}}{\text{kg}^\circ \text{K}}\right)} = 0.13355$$

Finally, using Eq. 2.46

$$\frac{c_p}{c_v} = [1 - 0.13355]^{-1} = 1.154$$

CHAPTER THREE

EXPERIMENTAL PROCEDURES

In this chapter the experimental apparatus and procedure for determining the isothermal compressibility and heat capacity ratios are discussed and explained. An analysis of errors in compressibility measurement is given. And the time for thermal equilibration of experiments is discussed at the end of the chapter.

3.1 Experimental Apparatus

Figure 3.1 is a schematic of the apparatus used in the isothermal compressibility measurement. The high pressure positive displacement pump displaces the fluid sample from the transfer vessel to the pressure vessel. The piston in the transfer vessel separates the hydraulic oil from the sample fluid. The high pressure valve A can isolate the pressure vessel from the transfer vessel and the pump. Valve B, the “micro-pump,” is a high pressure valve that provides sufficient volume change for measurement of compressibilities with the system.

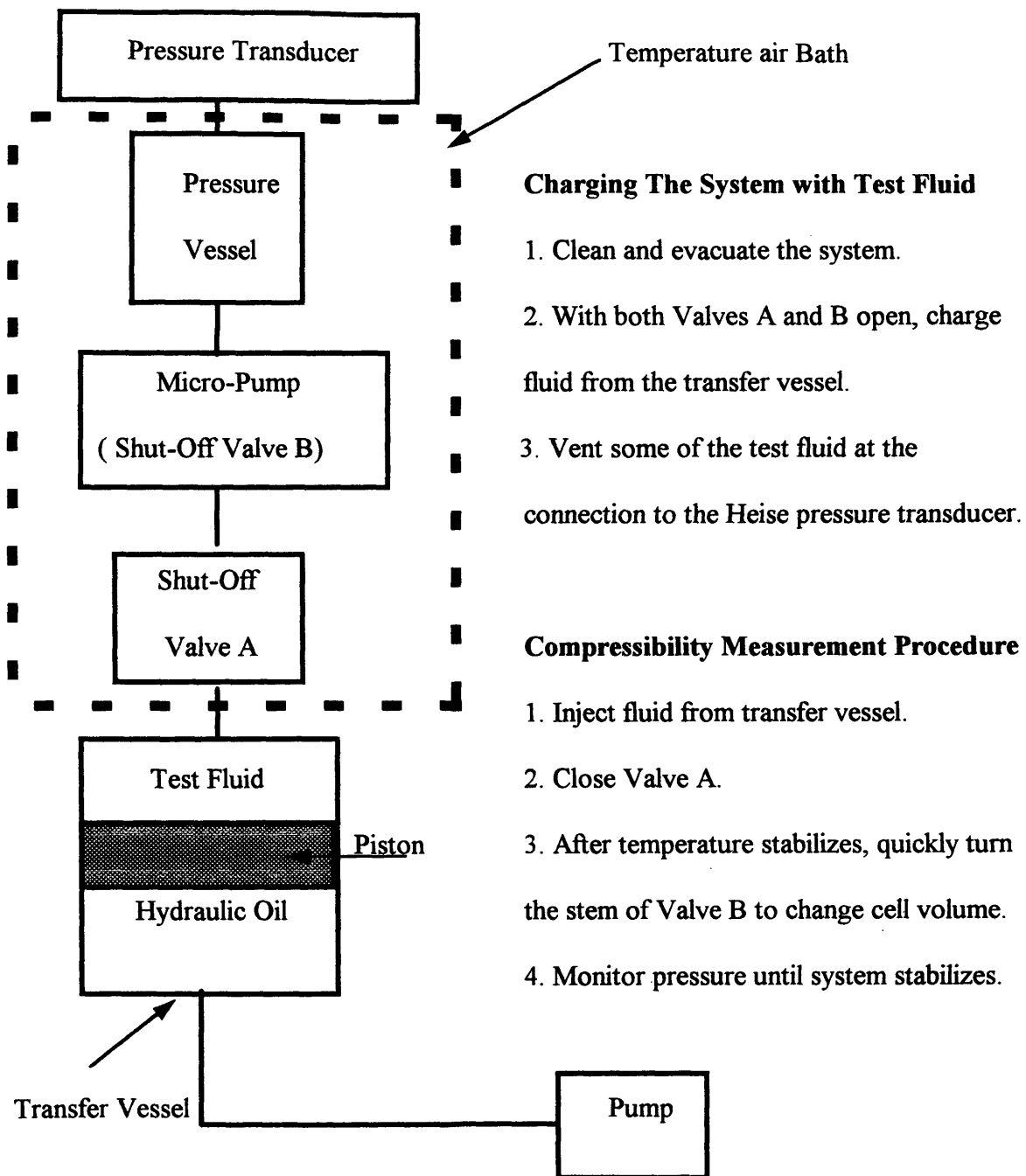


Figure 3.1 Schematic of Apparatus for Measuring Compressibility of Fluids.

The pressure vessel, valves A and B are inside a DB Robinson air bath for controlling temperatures. Temperatures up to 250°F are possible. All parts of the apparatus are designed for operation up to 10,000 psi.

The pressure vessel has an internal volume of about 40 cm³ of test fluid. The total sample volume of the apparatus is 42.7 cm³, including the pressure vessel, valve B, and the connecting tubes from valve A. The internal volume of the transfer vessel is 500 cm³. By turning the stem of the micro-pump, the maximum possible volume change is 0.076 cm³. To calculate the change in volume caused by turning the valve stem, the following equation is used:

$$\Delta v = \left(\frac{n}{24}\right)\left(\frac{\pi}{4}\right)D^2 \quad (3.1)$$

where,

Δv = change in volume, in³

n = number of turns,

24= threads per inch,

$\frac{n}{24}$ = inches of displacement, and,

D = diameter of the HIP valve stem =0.188 inches.

For all testing described in this thesis, the stem of valve B was turned four times, which provides the maximum volume change of 0.076 cm³. For this volume

change, the pressure changes sensed by the Heise transducer were typically 200 to 400 psi. With the apparatus of Fig. 3.1, compression or expansion tests were possible, depending on whether valve B was turned four revolutions to the closed position, or four revolutions to the open position.

The pressure in the test cell was very sensitive to temperature variations because the fluids examined in this research were all liquids. A cooling unit was added to the DB Robinson air bath to give better temperature control, especially at temperatures just above room temperature. When the air bath temperature was not stable, the observed pressure would wander as can be seen in Figure 3.2. Under such conditions, measurement of compressibility was not possible. Another example of the effects of poor temperature control is shown in Figure 3.3 for a pentane sample at 140°F.

Pressure Vs. Time (at a Variable Temperature Range 140-142.5oF)

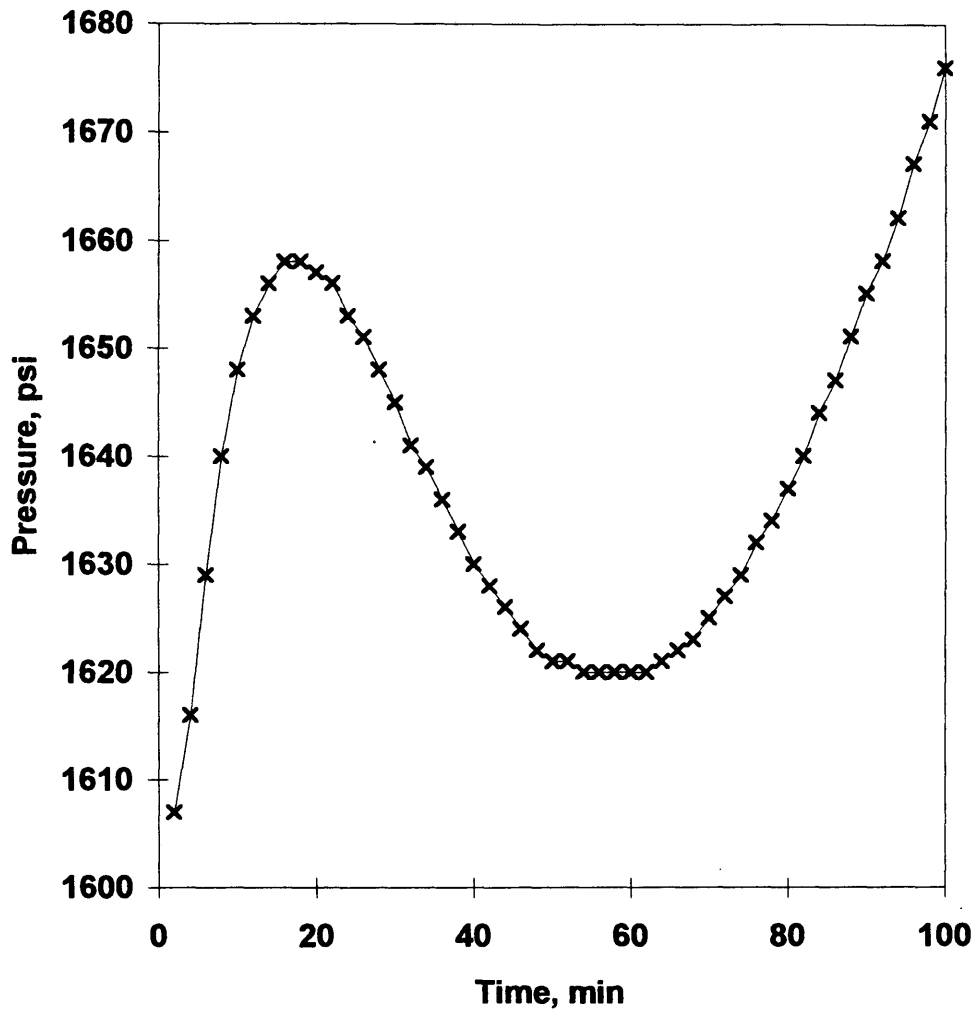


Figure 3.2 Pressure vs. Time for a Decane sample at range of 140-143°F.

**Pressure History for Both Compression and
Expansion Test with Pentane at 140°F**

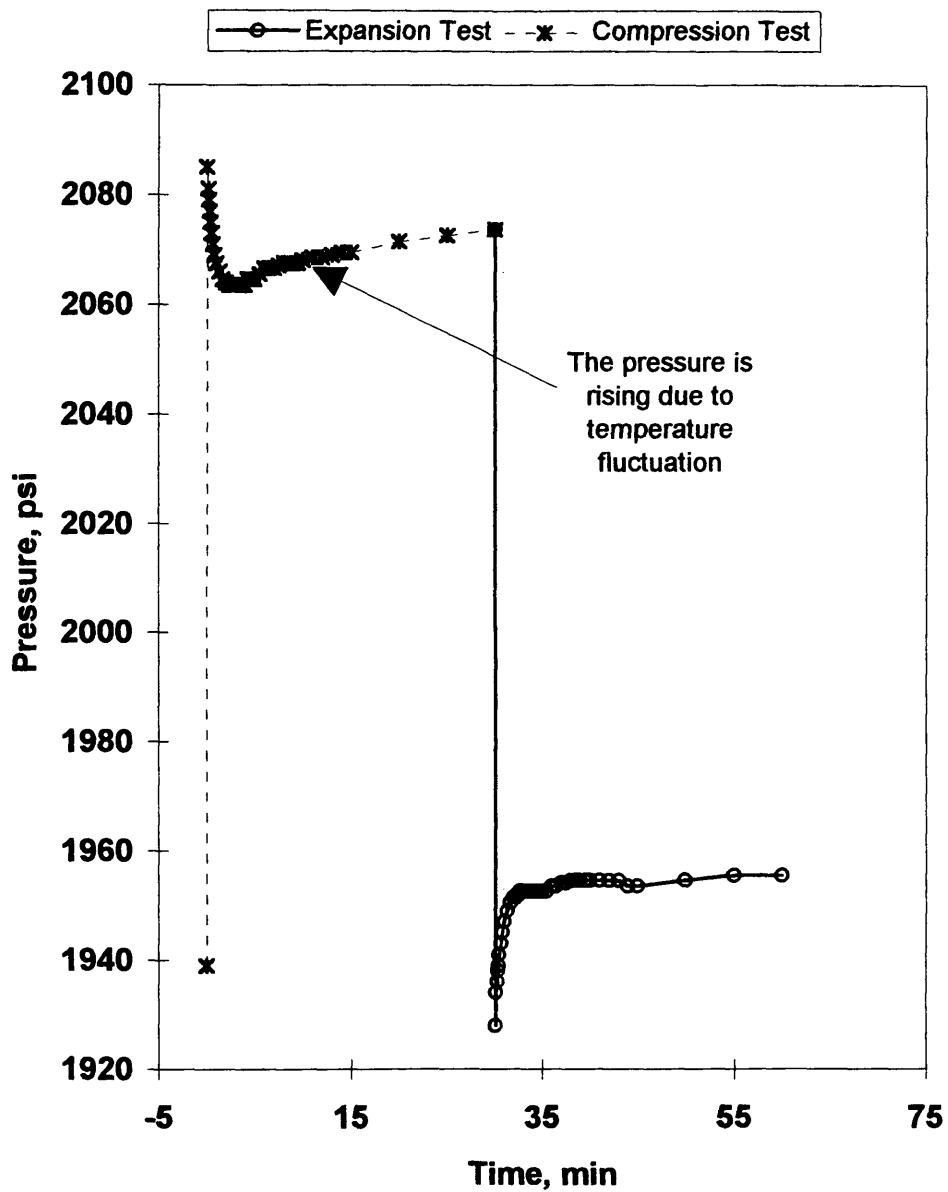


Figure 3.3 The effect of poor temperature control for Pentane sample at 140°F.

3.2 Experimental Procedure

Before starting an experiment, the system was purged of previous fluids by blowing air from the transducer connection through the pressure vessel and valves A and B. To do this, fittings were disconnected at the transducer and between Valve A and the transfer vessel. Then, with all fittings re-connected, a new fluid sample was charged from the transfer vessel to the pressure vessel with the high pressure positive displacement pump. The pressure vessel was vented at the connection to the pressure transducer to purge air from the system. Then, the system was isolated by shutting valve A. Then, the door of the air bath was closed, and time was allowed for thermal equilibration.

After temperature stabilized, the stem of valve B was turned quickly to change the volume inside the pressure vessel, and pressure was recorded for 10 to 30 minutes until it reached a stable value. All of these operations, including reading of pressures, were done manually. As of yet, the equipment has not been automated.

3.3 Dead Volume Error in Compressibility Measurement

A pressure transducer is an essential part of compressibility measurement. For reliable operation, most pressure transducers need to be located outside of a

temperature bath, particularly if the bath will operate at temperatures much above 100°F. At the start of this effort, there was concern for the effect on the accuracy of compressibility measurement of the dead volume of the transducer and the line leading to the transducer, both of which were located outside the air bath.

The analysis below demonstrates that this dead volume error could be minimized by making the ratio of the volume of the test system outside the temperature bath to the volume inside the temperature bath as small as possible.

The total volume of the system is the sum of the volumes inside and outside the air bath:

$$v_T = v_i + v_o \quad (3.2)$$

where,

v_T = total system volume, cm^3 ,

v_i = volume inside temperature bath, cm^3 ,

v_o = volume outside temperature bath, cm^3 .

The total compressibility of the system is defined by the response of the system pressure p to a change in volume:

$$c_T = -\frac{1}{v_T} \left(\frac{\partial v_T}{\partial p} \right)_T \quad (3.3)$$

Substituting Eq. 3.2 for v_T in Eq. 3.3, then

$$c_T = -\frac{1}{v_i + v_o} \left(\frac{\partial(v_i + v_o)}{\partial p} \right)_T \quad (3.4)$$

Multiplying Eq. 3.4 by $(v_i + v_o)$ and simplifying we get,

$$c_T(v_i + v_o) = -\left(\frac{\partial v_i}{\partial p} \right)_T - \left(\frac{\partial v_o}{\partial p} \right)_T \quad (3.5)$$

Now, c_i and c_o are introduced to represent the inside and outside isothermal compressibility:

$$c_i = -\frac{1}{v_i} \left(\frac{\partial v_i}{\partial p} \right)_T \quad (3.6)$$

and

$$c_o = -\frac{1}{v_o} \left(\frac{\partial v_o}{\partial p} \right)_T \quad (3.7)$$

Therefore, with Eqs. 3.6 and 3.7, Eq. 3.5 becomes

$$c_T(v_i + v_o) = c_i v_i + c_o v_o \quad (3.8)$$

Rearrangement of Eq. 3.8 gives the final expression:

$$c_i = c_T + (c_T - c_o) \frac{v_o}{v_i} \quad (3.9)$$

According to Eq. 3.9, if c_T and c_o differ by 10% and v_o is 10 % or less of v_i , then,

$$c_i V_i \cong c_T V_i \quad (3.10)$$

with an error of 1% or less.

3.4 Time for Thermal Equilibration

For design purposes, it was important to estimate the time for thermal equilibration of the apparatus during an experiment. Thermal equilibration is a significant factor in the measurement of isothermal compressibility, therefore, the thermal equilibration time is a necessary measurement. The time for thermal equilibration is a function of thermal diffusion and the distance over which temperatures must adjust. According to Bird *et al.* (1960) the time for thermal equilibration is approximately given by the following expression:

$$t = \frac{s^2}{D} \quad (3.11)$$

where,

t = time required for temperature stabilization, seconds (s),

s = distance of equilibration, cm,

D = thermal diffusivity, cm^2/s

Consider the following example for estimating the thermal equilibration time of a stainless steel vessel with a 0.5 cm thick wall. According to Kreith (1973) the thermal diffusivity for stainless steel is

$$D = 0.15 \frac{\text{ft}^2}{\text{hr}} \left(\frac{30.48 \text{cm}}{\text{ft}} \right)^2 \left(\frac{1 \text{hr}}{3600 \text{sec}} \right) = 0.0013 \frac{\text{cm}^2}{\text{s}}$$

Then, with Eq. 3.11, the time for equilibration across the steel wall is approximately 3 minutes:

$$t = \frac{S^2}{D} = \frac{(0.5 \text{cm})^2}{0.0013 \frac{\text{cm}^2}{\text{s}}} = 197 \text{ s}$$

From the above calculations, it can be concluded that a minimum of three minutes time is required for temperature stabilization across the stainless steel pressure vessel.

CHAPTER FOUR

EXPERIMENTAL RESULTS

In this chapter, examples of the observed pressure responses for four fluids are presented. The fluids are n-decane, Burly oil, de-ionized water, and n-pentane. Table 4.1 lists densities of the fluids. For each of the fluids, isothermal compressibility and heat capacity ratio measurements are reported for a variety of temperatures and pressures. Sonic velocities of the four fluids estimated from these are presented and compared with the literature values to the extent possible.

Table 4.1 Measured and literature density (ρ) values at room temperature (about 70 °F) for n-decane, de-ionized water, Burly oil, and n-pentane.

Tested Fluid	PE lab Measurement, g/cm ³	Literature, g/cm ³
Decane	0.7296	0.7342 ¹
Burly oil	0.7970	N/A
De-ionized water	0.9960	0.9982 ²
n-Pentane	0.6230	0.6311 ¹

¹ McCain, 1990, Table A1, p. 493.

² Weast, 1971, p. F-11.

4.1 Decane

Table 4.2 contains the isothermal compressibility values and heat capacity ratio measurements labeled “PE lab” for the n-decane sample at different temperatures and pressures. As can be seen, the n-decane isothermal compressibilities and heat capacity ratios compare well with the literature values (Vargaftik, 1983) listed in the table for most cases. As can be seen in Figures 4.1-4.8, compression and expansion tests were performed for each pressure and temperature. Procedures for these tests are described in Section 3.1. Figure 4.9

shows a graphical comparison of sonic velocities measured in the PE laboratory with those calculated from Vargaftik (1983).

Table 4.3 compares the sonic velocities calculated using Eq. 2.12 for decane as estimated from the data in Table 4.2 with densities from Table 4.1. Also shown in Table 4.3 are measurements of the sonic velocity reported by Prof. M. L. Batzle (1996), labeled “GP lab”.

Pressure histories for decane were recorded for both compression and expansion tests; most of the results were satisfactory. However, in some experiments the pressure did not stabilize to a constant value, as can be seen in Fig. 4.1 and Fig. 4.4. As shown in both figures, pressure is not leveling to a constant value, but is slowly rising. The pressure rise was mostly likely a result of increasing temperature. The temperature was increasing due to the cooling fan motor operation. This problem was noticed and fixed in the early stages of experimentation by adding a refrigeration system to have better air bath temperature control.

Table 4.2 Measured and literature isothermal compressibilities and heat capacity ratios for n-decane.

Temperature, °C °F		Test Method	Pressure, MPa psi		Isothermal Compressibility,				Heat Capacity Ratio	
					PE lab, $\times 10^6$		Vargaftik, $\times 10^6$		PE lab	Vargaftik
			MPa	psi	MPa ⁻¹	psi ⁻¹	MPa ⁻¹	psi ⁻¹		
22.4 (Fig. 4.1)	72	Comp.	11.46	1662	970	6.69	N/A		1.153	N/A
		Exp.	11.45	1661	969	6.68	N/A		1.162	N/A
22.4 (Fig. 4.2)	72	Comp.	13.87	2012	903	6.23	N/A		1.084	N/A
		Exp.	13.86	2010	895	6.17	N/A		1.104	N/A
40 (Fig. 4.3)	104	Comp.	5.21	756	1327	9.15	1072	7.39	1.103	1.152
		Exp.	5.20	754	1301	8.97	1137	7.84	1.076	1.174
40 (Fig. 4.4)	104	Comp.	9.24	1340	1166	8.04	870	6.00	1.109	1.194
		Exp.	9.22	1338	1150	7.93	983	6.78	1.076	1.174
60 (Fig. 4.5)	140	Comp.	3.62	525	1395	9.62	2407	16.6	1.198	1.169
		Exp.	3.62	525	1356	9.35	2552	17.6	1.129	1.165
60 (Fig. 4.6)	140	Comp.	25.63	3717	1057	7.29	1122	7.74	1.138	1.248
		Exp.	25.60	3712	1018	7.02	1177	8.12	1.113	1.247
80 (Fig. 4.7)	176	Comp.	3.58	519	1581	10.9	2204	15.2	1.174	1.137
		Exp.	3.55	515	1508	10.4	2451	16.9	1.091	1.133
80 (Fig. 4.8)	176	Comp.	40.47	5868	976	6.73	N/A		1.12	N/A
		Exp.	40.46	5866	893	6.16	N/A		1.11	N/A

Comp. = compression,

Exp. = expansion,

N/A = not available.

Table 4.3 Calculated sonic velocity of n-decane for both literature obtained and laboratory measured data.

Temperature,		Test Method	Pressure,		Sonic velocity					
°C	F		MPa	psi	PE lab		Vargaftik		GP lab	
					m/s	ft/s	m/s	ft/s	m/s	ft/s
22.4	72	Comp.	11.46	1662	1282	4212	N/A		1319	4328
		Exp.	11.45	1661	1301	4269	N/A		1318	4324
22.4	72	Comp.	13.87	2012	1276	4187	N/A		1300	4265
		Exp.	13.86	2010	1282	4206	N/A		1300	4265
40	104	Comp.	5.21	756	1067	3501	1210	3970	1263	4144
		Exp.	5.20	754	1065	3494	1186	3891	1263	4144
40	104	Comp.	9.24	1340	1142	3760	1367	4485	1281	4203
		Exp.	9.22	1338	1132	3714	1275	4183	1281	4203
60	140	Comp.	3.62	525	1085	3560	813	2667	N/A	
		Exp.	3.62	525	1086	3563	789	2589	N/A	
60	140	Comp.	25.63	3717	1214	3983	1231	4039	1374	4508
		Exp.	25.60	3712	1224	4016	1201	3940	1373	4505
80	176	Comp.	3.58	519	1011	3317	839	2753	N/A	
		Exp.	3.55	515	996	3268	794	2605	N/A	
80	176	Comp.	40.47	5868	1254	4114	N/A		1450	4757
		Exp.	40.46	5866	1305	4282	N/A		1450	4757

**Pressure History for Both Compression and
Expansion Test with Decane at 72°F**

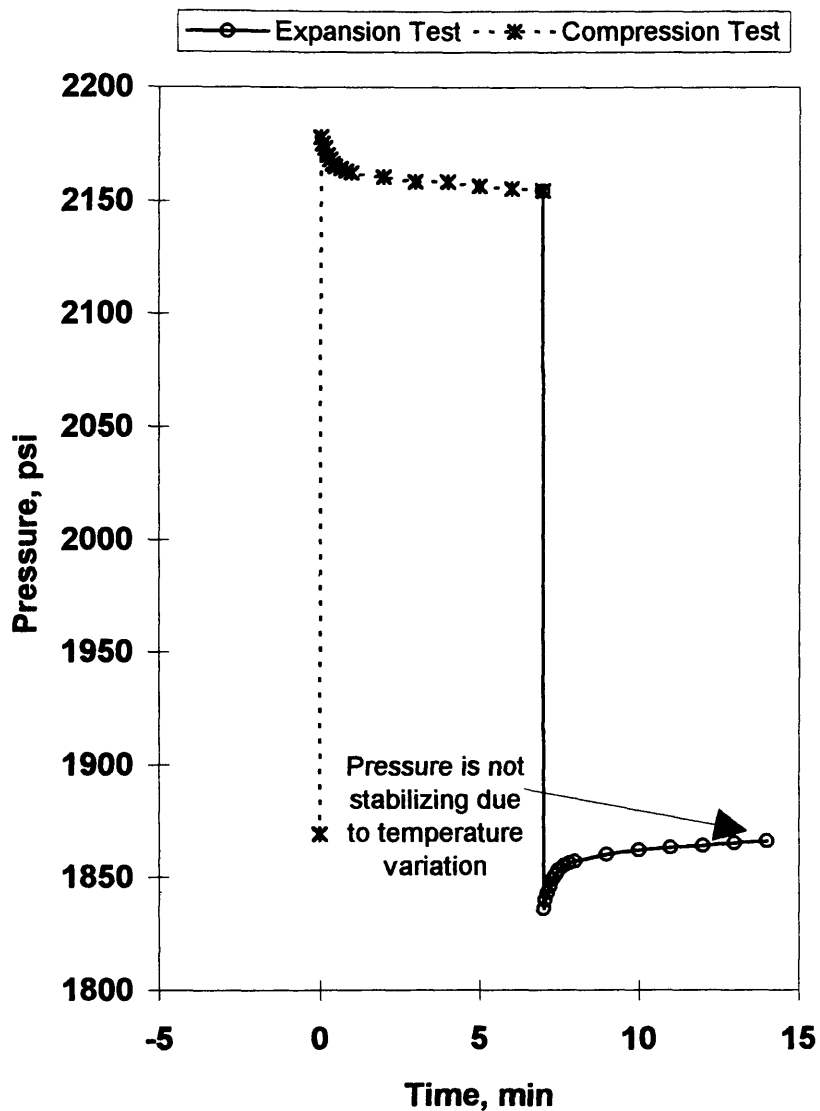


Figure 4.1 Pressure history for Decane sample at 72°F (Run 1).

**Pressure History for Both Compression and
Expansion Test with Decane at 72°F**

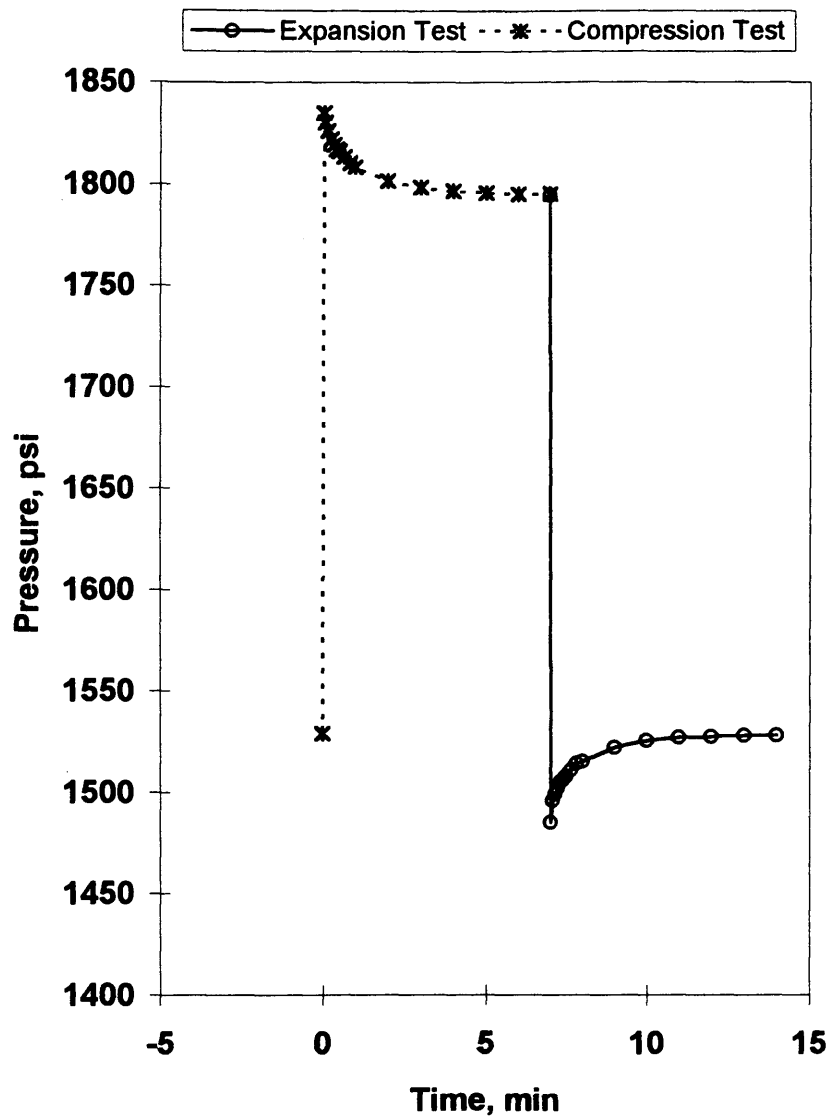


Figure 4.2 Pressure history for Decane sample at 72°F (Run 2).

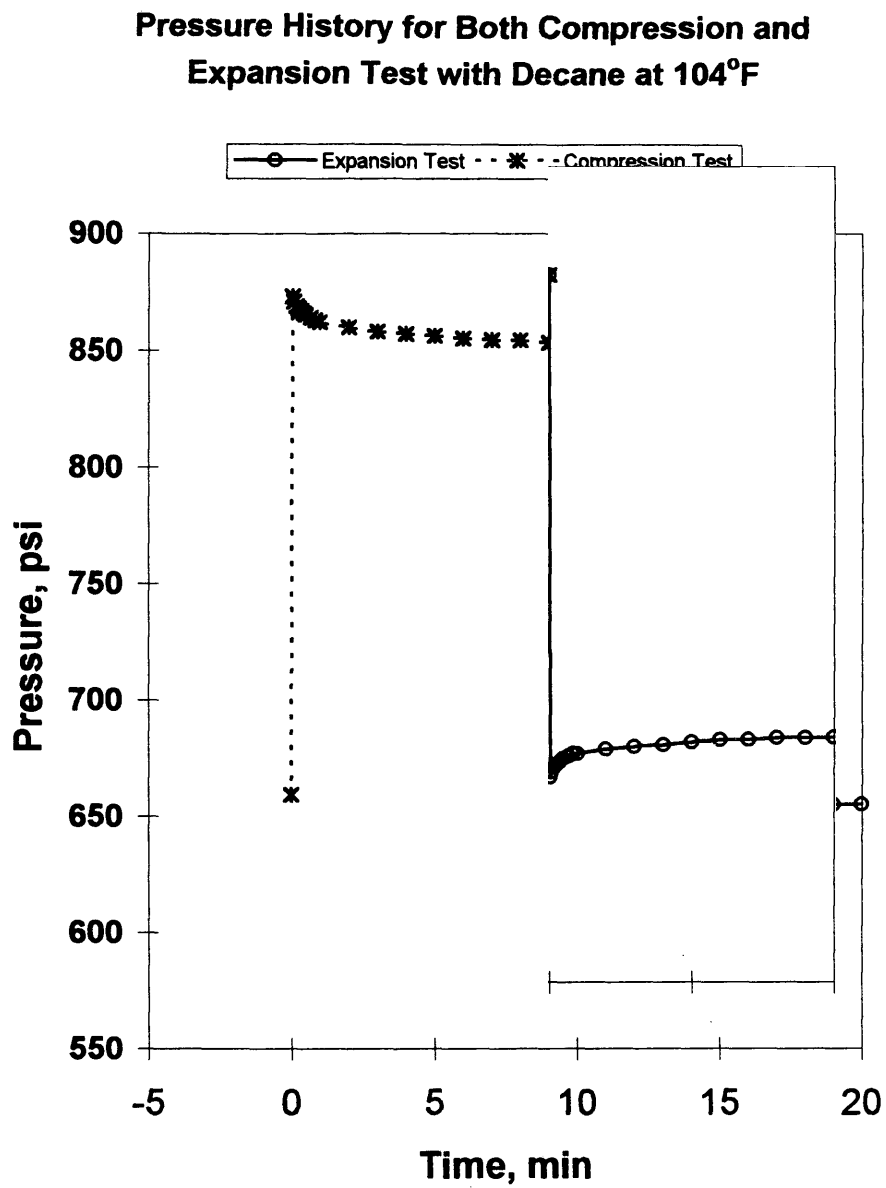


Figure 4.3 Pressure history for Decane sample at 104°F (Run1).

**Pressure History for Both Compression and
Expansion Test with Decane at 104°F**

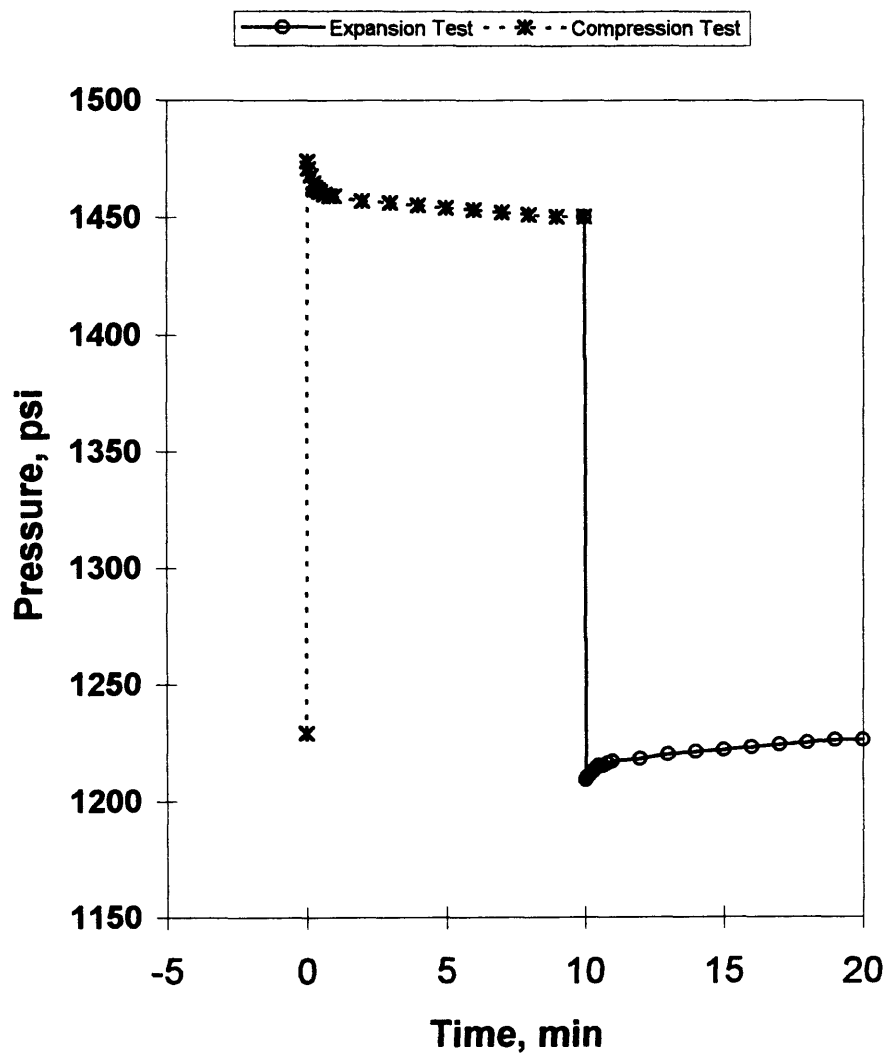


Figure 4.4 Pressure history for Decane sample at 104°F (Run2).

**Pressure History for Both Compression and
Expansion Test with Decane at 140°F**

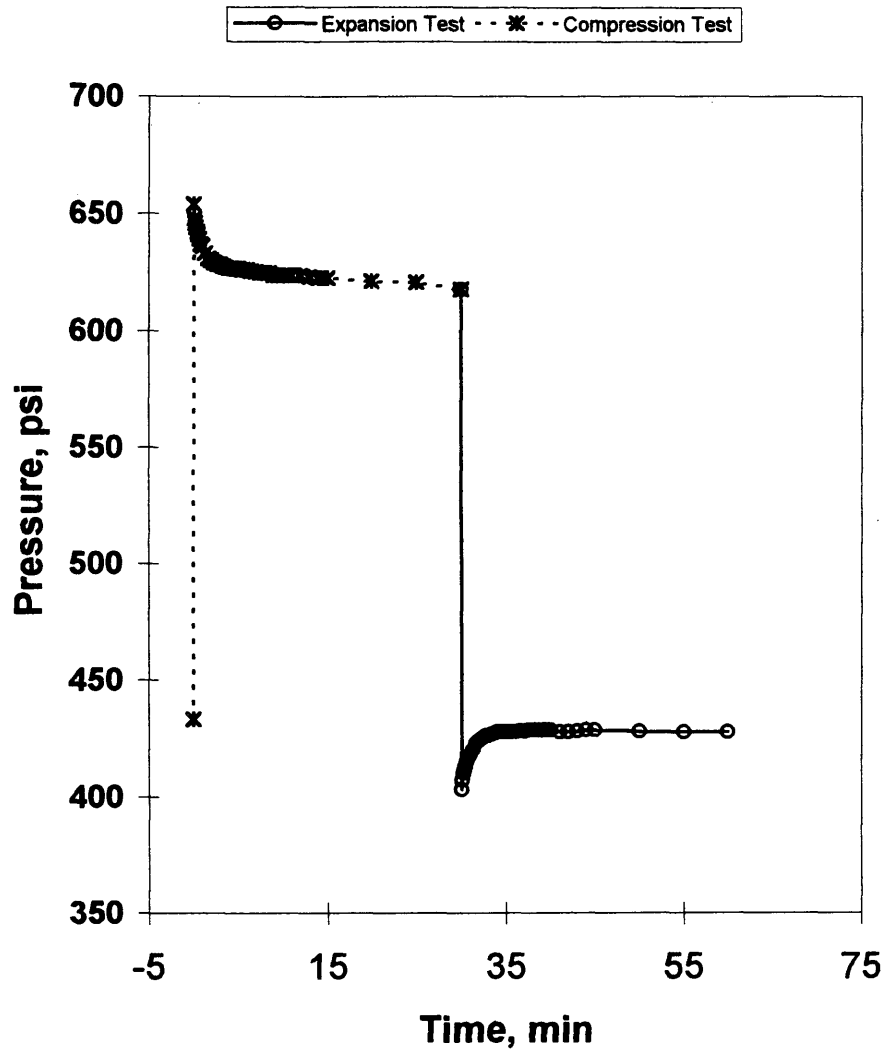


Figure 4.5 Pressure history for Decane sample at 140°F (Run1).

**Pressure History for Both Compression and
Expansion Test with Decane at 140°F**

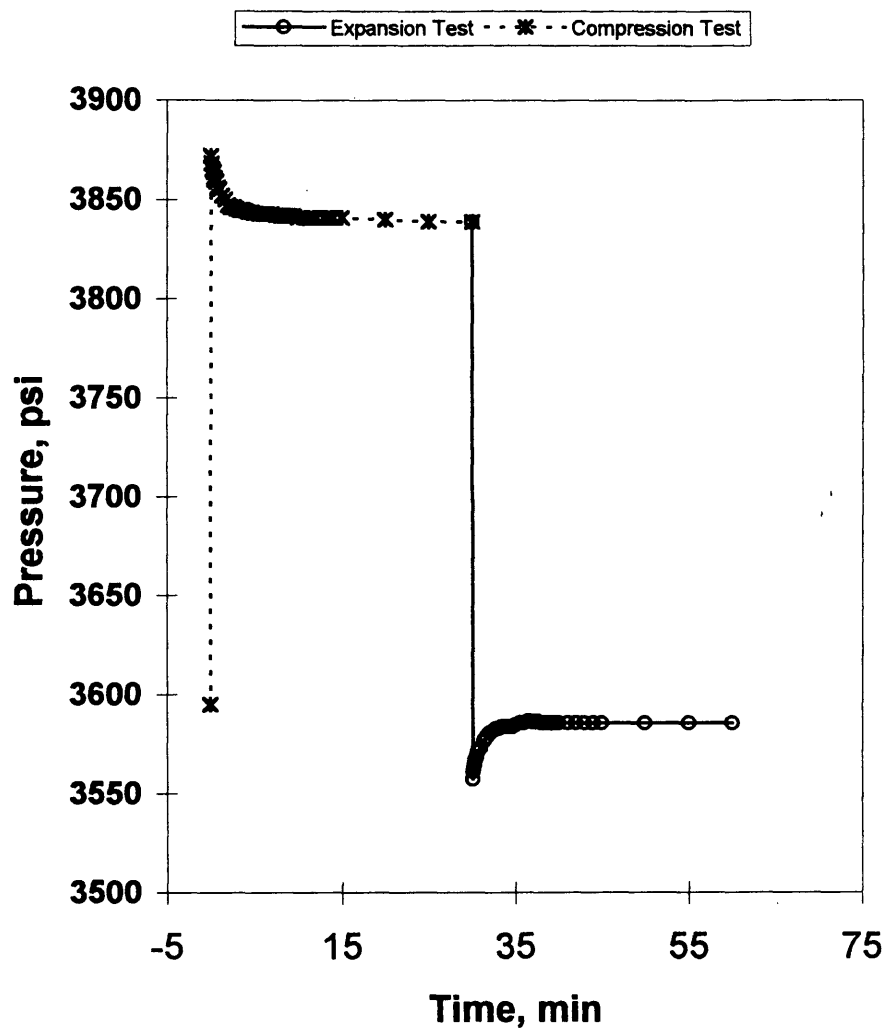


Figure 4.6 Pressure history for Decane sample at 140°F (Run2).

Pressure History for Both Compression and
Expansion Test with Decane at 176°F

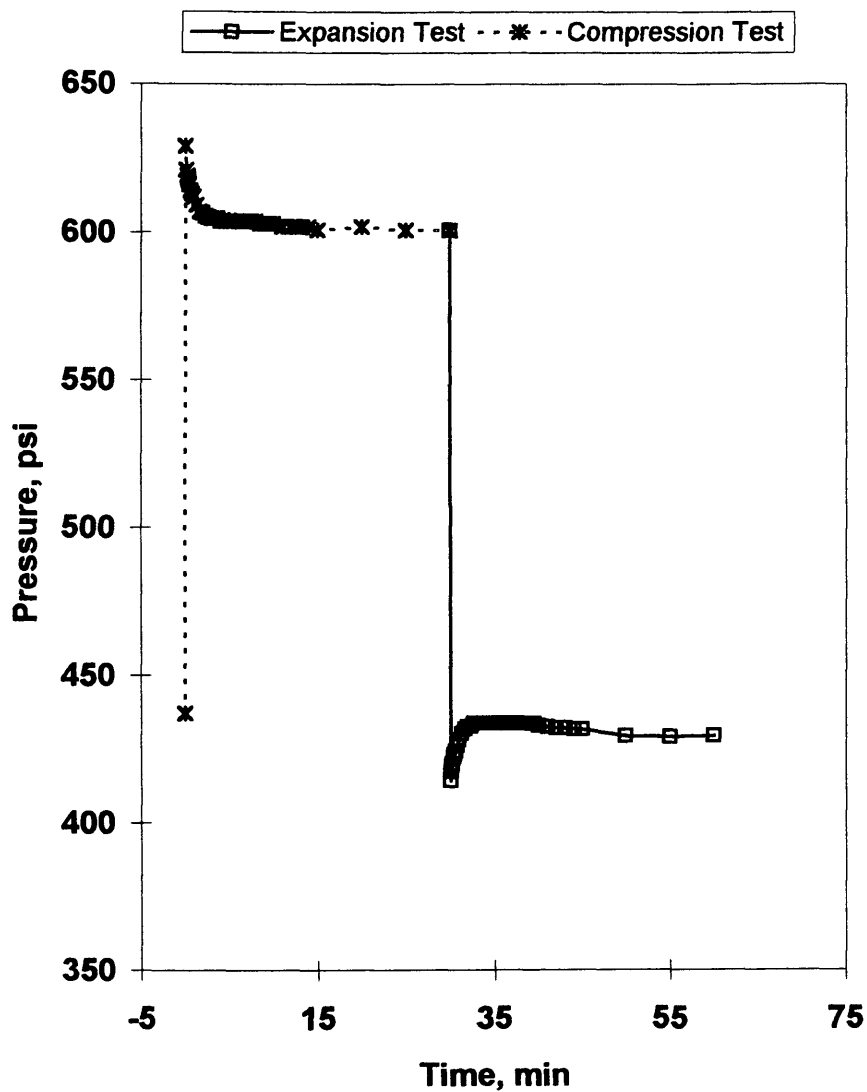


Figure 4.7 Pressure history for Decane sample at 176°F (Run1).

Pressure History for Both Compression and
Expansion Test with Decane at 176°F

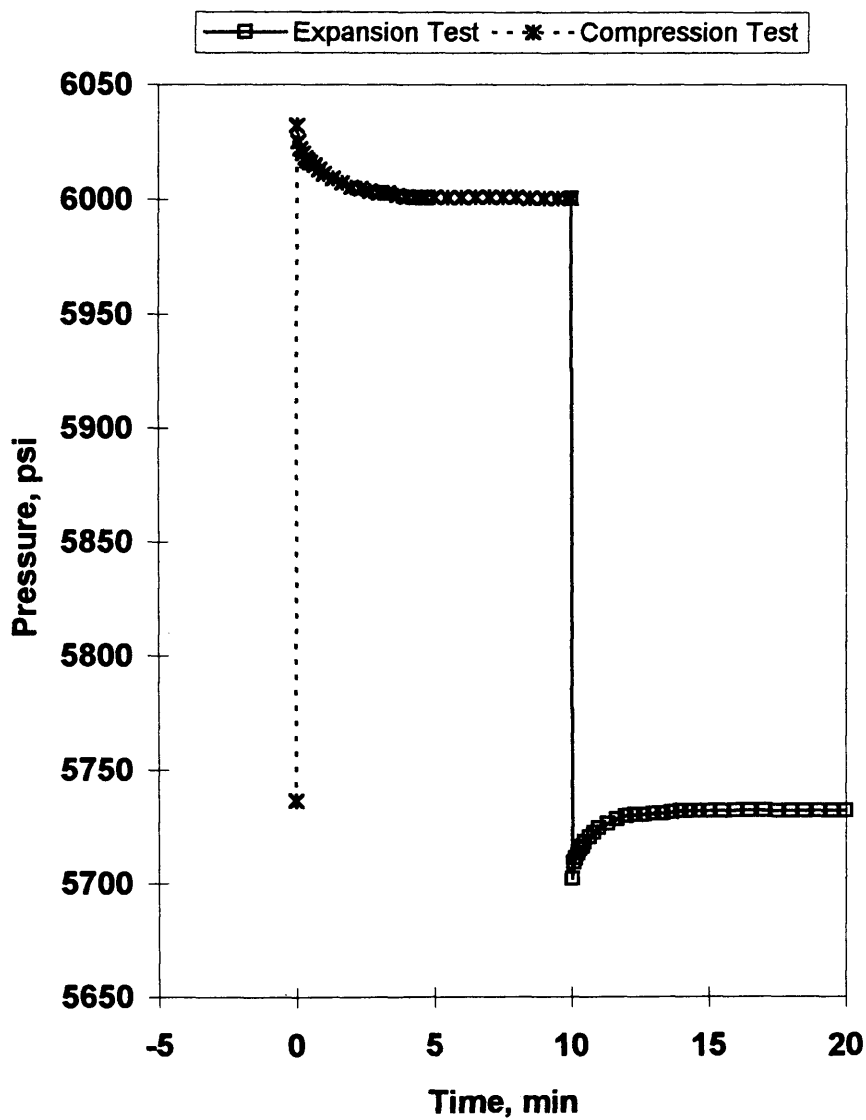


Figure 4.8 Pressure history for Decane sample at 176°F (Run2).

Comparison of Measured and Literature values Sonic Velocity for n-decane

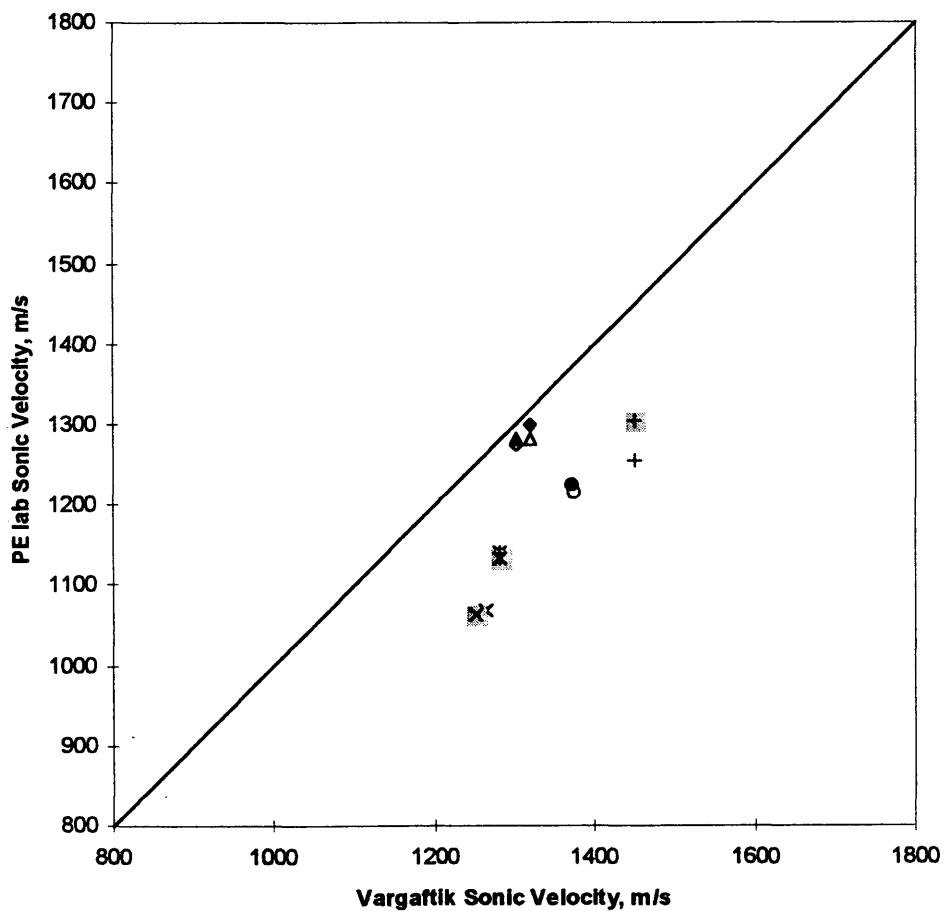
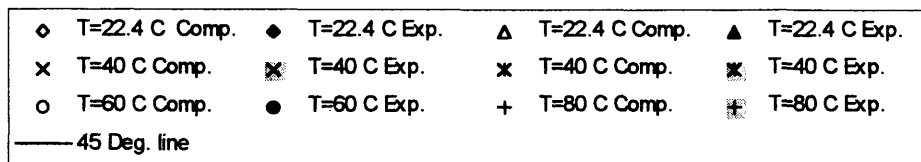


Figure 4.9 Sonic velocity values for n-decane from Vargaftik(1983) and the PE laboratory.

4.2 Burly Oil

Burly Oil was selected for tests in the Petroleum Engineering Department and the Geophysics Department because a substantial quantity of the oil was readily available. Table 4.4 contains isothermal compressibilities, heat capacity ratios, and sonic velocities. Sonic velocities from both laboratories show reasonable agreement.

Table 4.4 Measured isothermal compressibilities, heat capacity ratios, and sonic velocities for Burly oil sample at 40°C =104 °F.

Test Method	Pressure,		Isothermal Compressibility, x 10 ⁶		Heat Capacity Ratio	Sonic Velocity			
	MPa	psi	MPa ⁻¹	psi ⁻¹		PE lab		GP lab	
						m/s	ft/s	m/s	ft/s
Comp.	7.91	1147	937	6.46	1.153	1243	4078	1304	4278
Exp.	7.88	1143	931	6.42	1.132				
Comp.	10.96	1589	899	6.46	1.134	1258	4127	1319	4328
Exp.	10.96	1589	899	6.42	1.136				
Comp.	15.70	2277	870	6.00	1.149	1287	4124	1342	4403
Exp.	15.68	2273	848	5.85	1.120				

**Pressure History for Both Compression and
Expansion Test with Burly Oil Sample at 104°F**

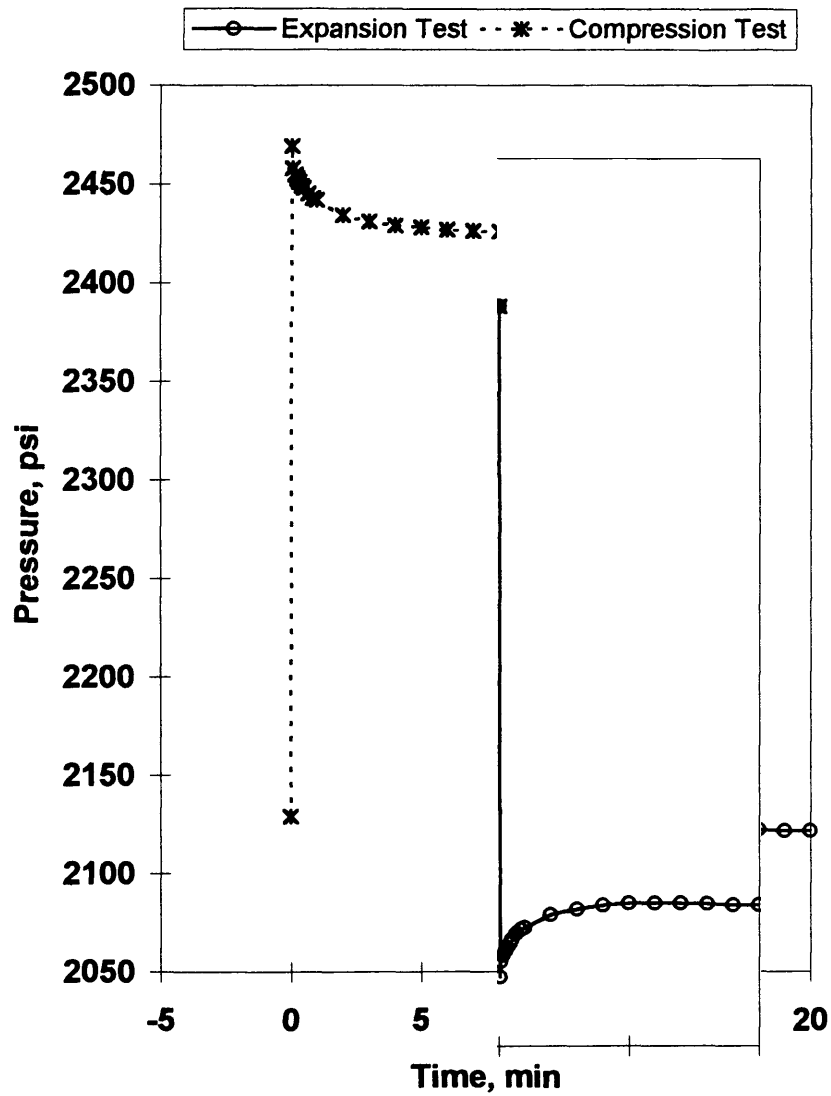


Figure 4.10 Pressure history for Burly oil sample at 104°F (Run 1).

**Comparisons of Measured and Literature values Sonic Velocity for
Burly Oil**

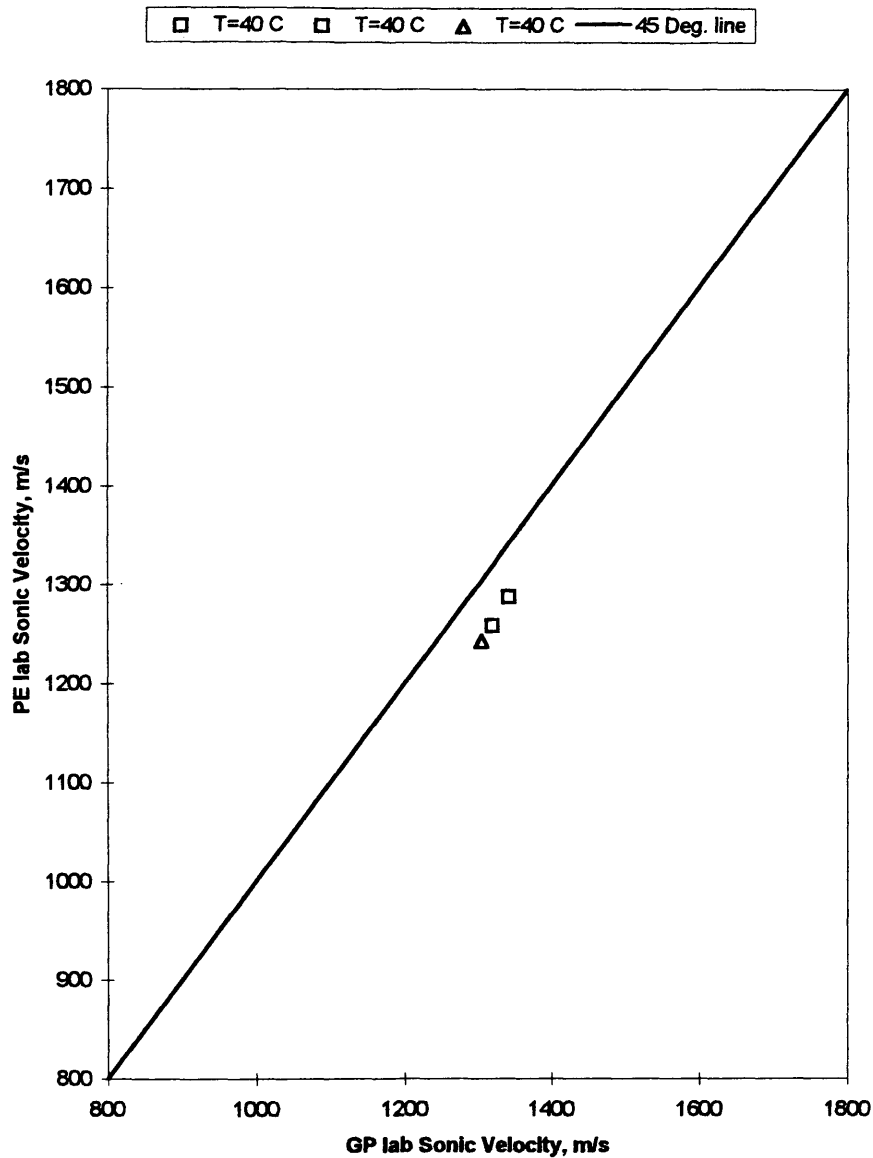


Figure 4.13 Sonic velocity values for Burly Oil from Geophysics and Petroleum laboratory measurements.

4.3 De-Ionized Water

Table 4.5 contains isothermal compressibilities, and heat capacity ratios for de-ionized water. The measured physical properties from Table 4.5 are used to calculate the sonic velocity for the de-ionized water, and reported in Table 4.6.

Figures 4.14-4.21 represent de-ionized water experiments for different temperatures and pressures. Figure 4.15 represents a compression and expansion test for de-ionized water at 71 °F and 1100-1700 psi. Unlike the pressure histories in the previous sections on decane and Burly oil, the pressure curves become flat right after compressing or expanding the system. Such behavior indicates that the heat capacity ratio is very close to unity. For some of the experiments, the pressure histories for expansion tests indicate heat capacity ratios less than unity. Such results must be erroneous, because the heat capacity ratio must be greater than or equal to unity.

The pressure histories for water develop some curvature at higher temperature and pressure (Figures 4.18 to 4.21), which indicates that the heat capacity ratios are departing substantially from unity.

Figures 4.22 and 4.23 represent water heat capacity ratios from the literature as functions of pressure and temperature respectively. Figure 4.22 shows that heat capacity ratios are rather insensitive to pressure, while Figure 4.23 shows

a stronger sensitivity to temperature. Figure 4.23 shows that the heat capacity ratio increases with temperature as demonstrated in the pressure histories of Figures 4.14 to 4.21. Figure 4.24 represents a comparison of sonic velocity values from available literature, calculated and laboratory measured.

Table 4.5 Measured and literature isothermal compressibilities and heat capacity ratios for de-ionized water.

Temperature °C	°F	Test Method	Pressure,		Isothermal Compressibility, x 10 ⁶						Heat Capacity Ratio	
			MPa	psi	PE lab		Lit. ¹		Lit. ²		PE lab	Lit. ³
			MPa	psi	MPa ⁻¹	psi ⁻¹	MPa ⁻¹	psi ⁻¹	MPa ⁻¹	psi ⁻¹		
21.7 (Fig. 4.12)	71	Comp.	9.59	1391	484	3.34	412	2.84	N/A		1.014	1.018
		Exp.	7.57	1388	477	3.29	412	2.84	N/A		0.974	1.018
21.7 (Fig. 4.13)	71	Comp.	34.38	4986	455	3.14	458	3.16	N/A		1.019	1.020
		Exp.	34.47	4998	468	3.23	458	3.16	N/A		0.997	1.020
37.8 (Fig. 4.14)	100	Comp.	21.01	3046	451	3.11	426	2.94	N/A		1.020	1.025
		Exp.	21.01	3046	451	3.11	426	2.94	N/A		1.017	1.025
37.8 (Fig. 4.15)	100	Comp.	21.28	3085	455	3.14	423	2.92	N/A		1.027	1.025
		Exp.	21.23	3079	448	3.09	423	2.92	N/A		1.013	1.025
65.6 (Fig. 4.16)	150	Comp.	38.07	5520	429	2.96	392	2.70	N/A		1.039	1.065
		Exp.	38.07	5520	429	2.96	392	2.70	N/A		1.02	1.065
65.6 (Fig. 4.17)	150	Comp.	38.2	5539	431	2.97	392	2.70	N/A		1.041	1.065
		Exp.	38.2	5539	429	2.96	392	2.70	N/A		1.041	1.065
93.4 (Fig. 4.18)	200	Comp.	35.16	5098	434	2.99	432	2.98	434	2.99	1.008	1.090
		Exp.	35.15	5097	435	3.00	432	2.98	434	2.99	1.022	1.090
93.4 (Fig. 4.19)	200	Comp.	35.39	5132	452	3.12	431	2.97	434	2.99	1.067	1.09
		Exp.	35.38	5130	450	3.10	431	2.97	438	3.02	1.06	1.090

¹ McCain, Figure (16.12), p. 453.

² McCain, Equation (B-70) p. 526.

³ Helgeson, and Kirkham, American Journal of Science p.1180.

Table 4.6 Calculated sonic velocity of de-ionized water for both literature obtained and laboratory measured data.

Temperature		Test Method	Pressure,		Sonic velocity					
°C	°F		MPa	psi	PE lab		Helgeson		Wilson	
					m/s	ft/s	m/s	ft/s	m/s	ft/s
21.7	71	Comp.	9.59	1391	1450	4757	1589	5214	1503	4931
		Exp.	7.57	1388	1449	4754	1589	5214	1503	4931
21.7	71	Comp.	34.38	4986	1450	4757	1588	5210	1547	5076
		Exp.	34.47	4998	1445	4741	1588	5210	1547	5076
37.8	100	Comp.	21.01	3046	1507	4944	1557	5109	1560	5118
		Exp.	21.01	3046	1505	4938	1557	5109	1560	5118
37.8	100	Comp.	21.28	3085	1505	4938	1557	5109	1561	5122
		Exp.	21.23	3079	1507	4944	1557	5109	1561	5122
65.6	150	Comp.	38.07	5520	1559	5115	1657	5437	1591	5220
		Exp.	38.07	5520	1545	5069	1657	5437	1591	5220
65.6	150	Comp.	38.2	5539	1558	5112	1657	5437	1592	5223
		Exp.	38.2	5539	1561	5122	1657	5437	1592	5223
93.4	200	Comp.	35.16	5098	1527	5010	1587	5207	1615	5299
		Exp.	35.15	5097	1525	5004	1587	5207	1615	5299
93.4	200	Comp.	35.39	5132	1539	5049	1587	5207	1616	5299
		Exp.	35.38	5130	1539	5049	1587	5207	1616	5299

**Pressure History for Both Compression and
Expansion Test with De-ionized water sample at
71°F**

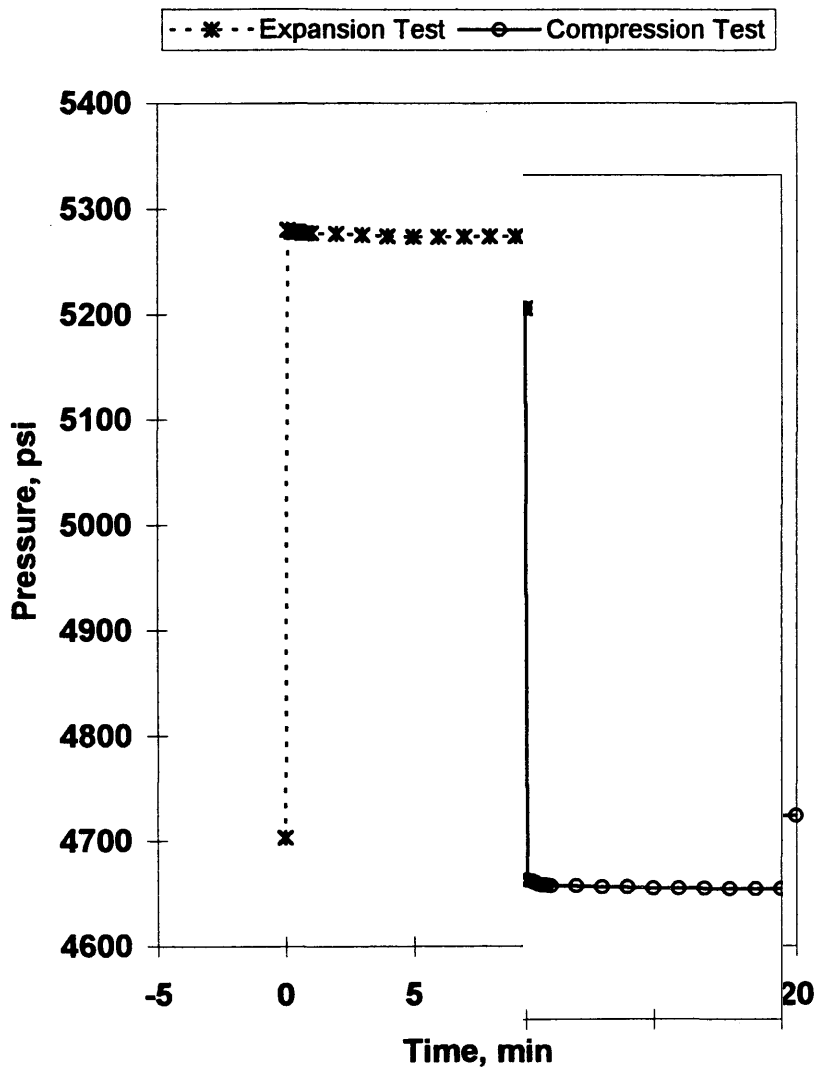


Figure 4.14 Pressure history for De-ionized water sample at 71°F (Run 1).

**Pressure History for Both Compression and
Expansion Test with De-ionized water sample at
71°F**

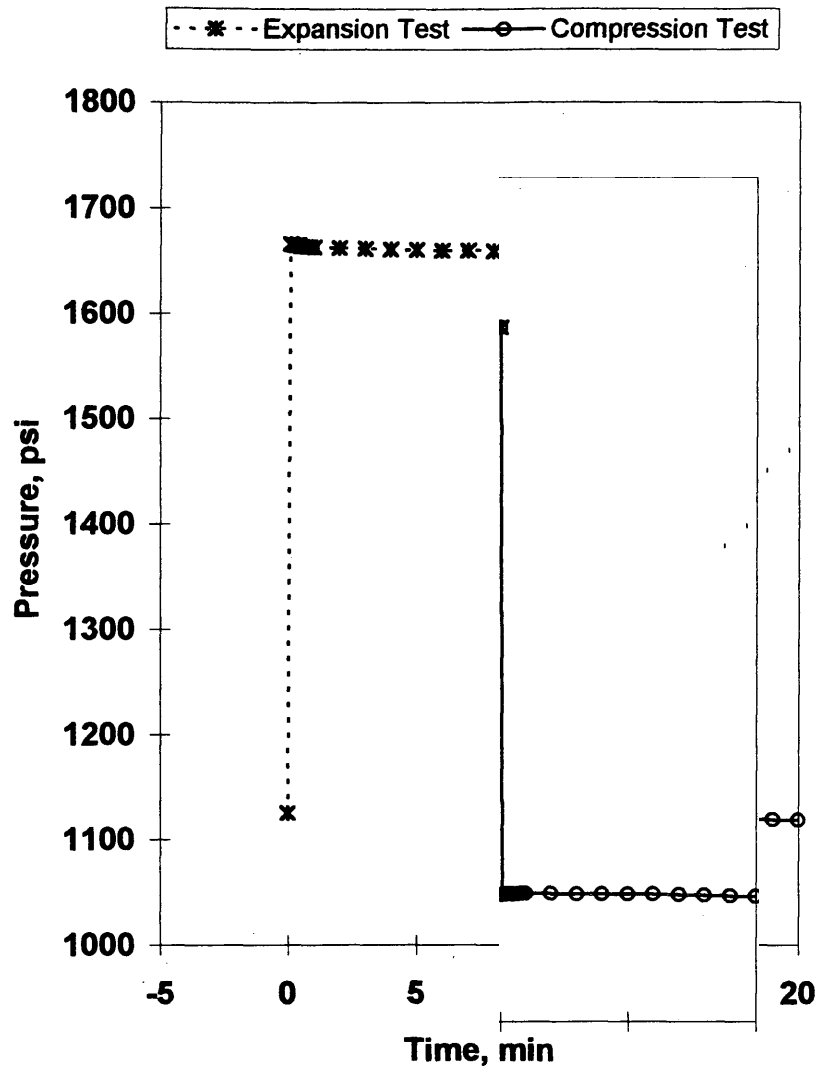


Figure 4.15 Pressure history for De-ionized water sample at 71°F (Run 2).

**Pressure History for Both Compression and
Expansion Test with De-ionized water sample at
100°F**

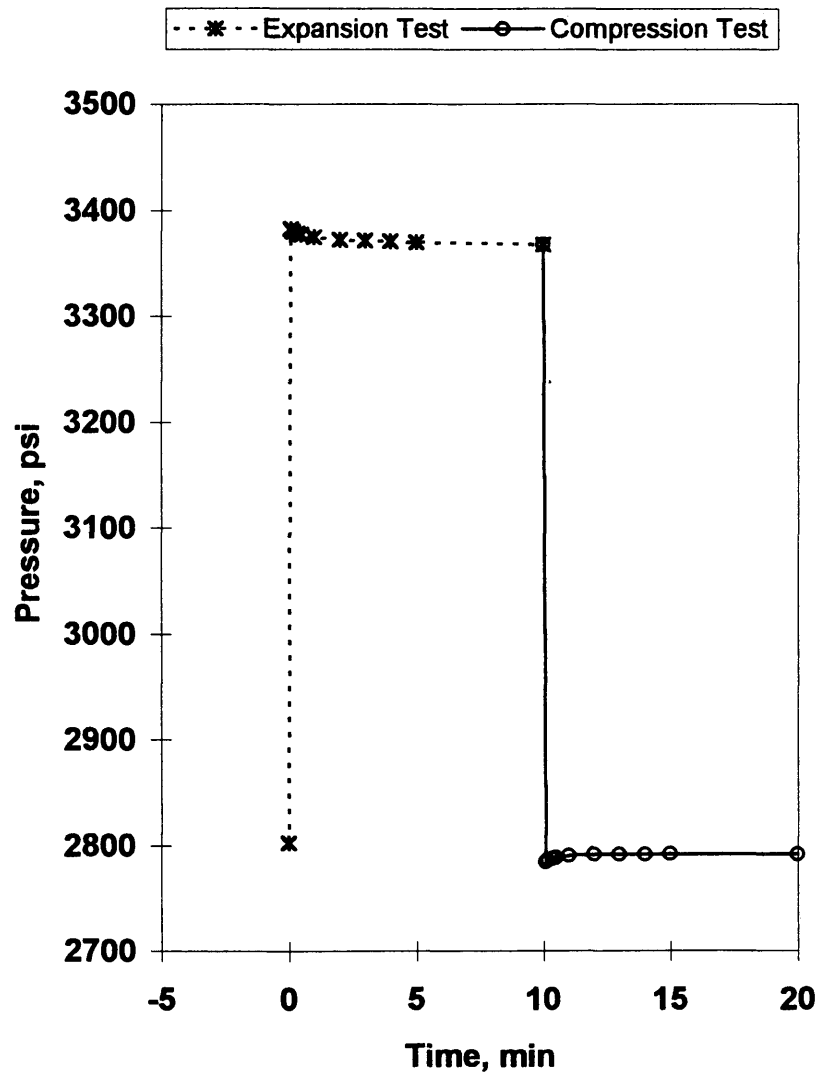


Figure 4.16 Pressure history for De-ionized water sample at 100°F (Run1).

**Pressure History for Both Compression and
Expansion Test with De-ionized water sample at
100°F**

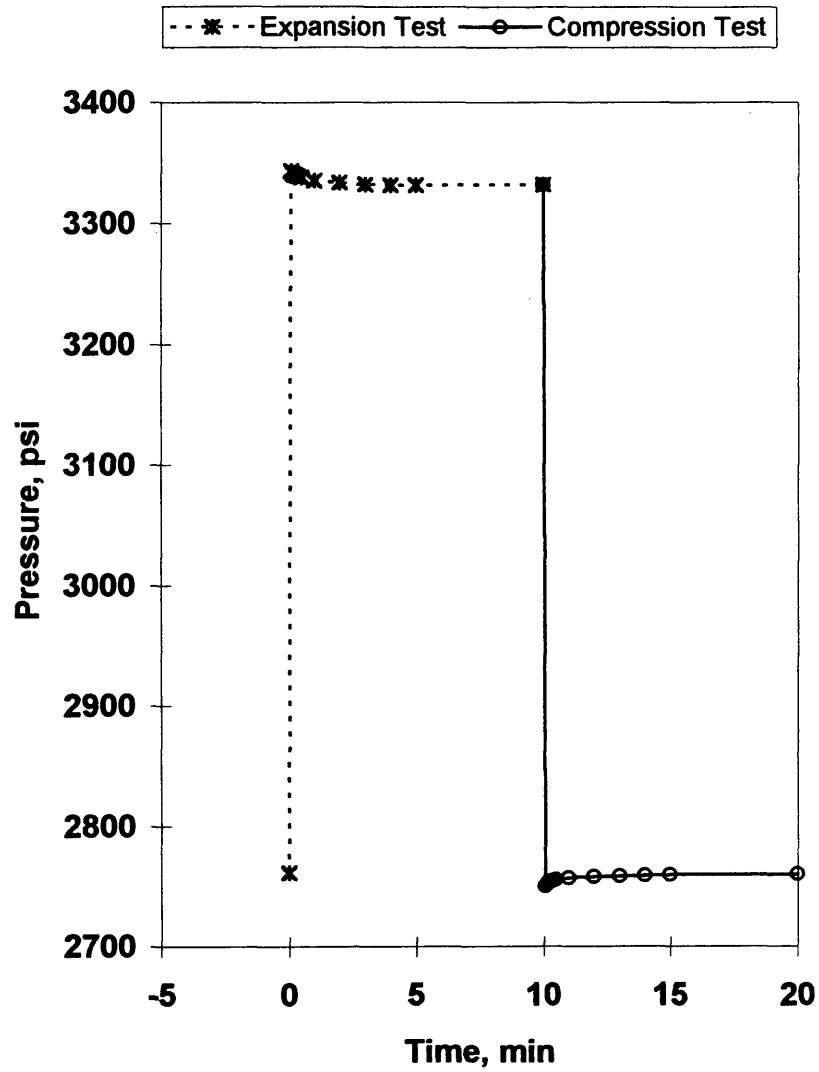


Figure 4.17 Pressure history for De-ionized water sample at 100°F(Run 2).

**Pressure History for Both Compression and
Expansion Test with De-ionized water sample at
150°F**

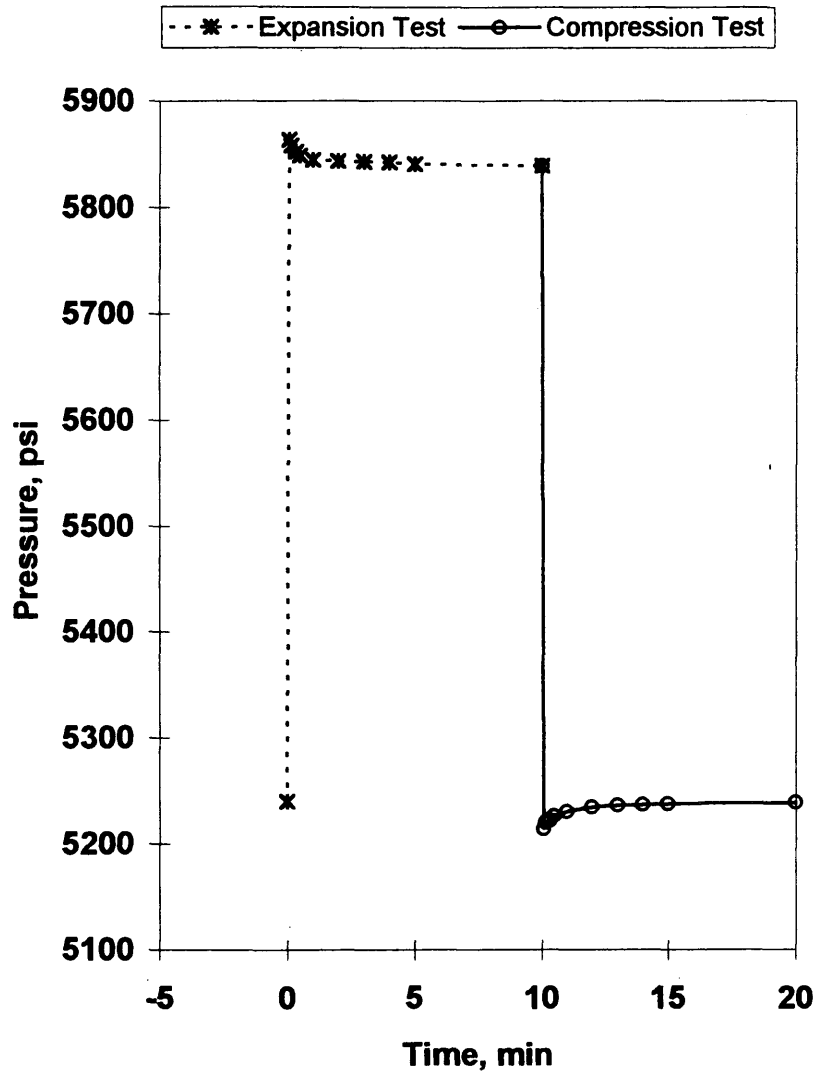


Figure 4.18 Pressure history for De-ionized water sample at 150°F(Run 1).

**Pressure History for Both Compression and
Expansion Test with De-ionized water sample at
150°F**

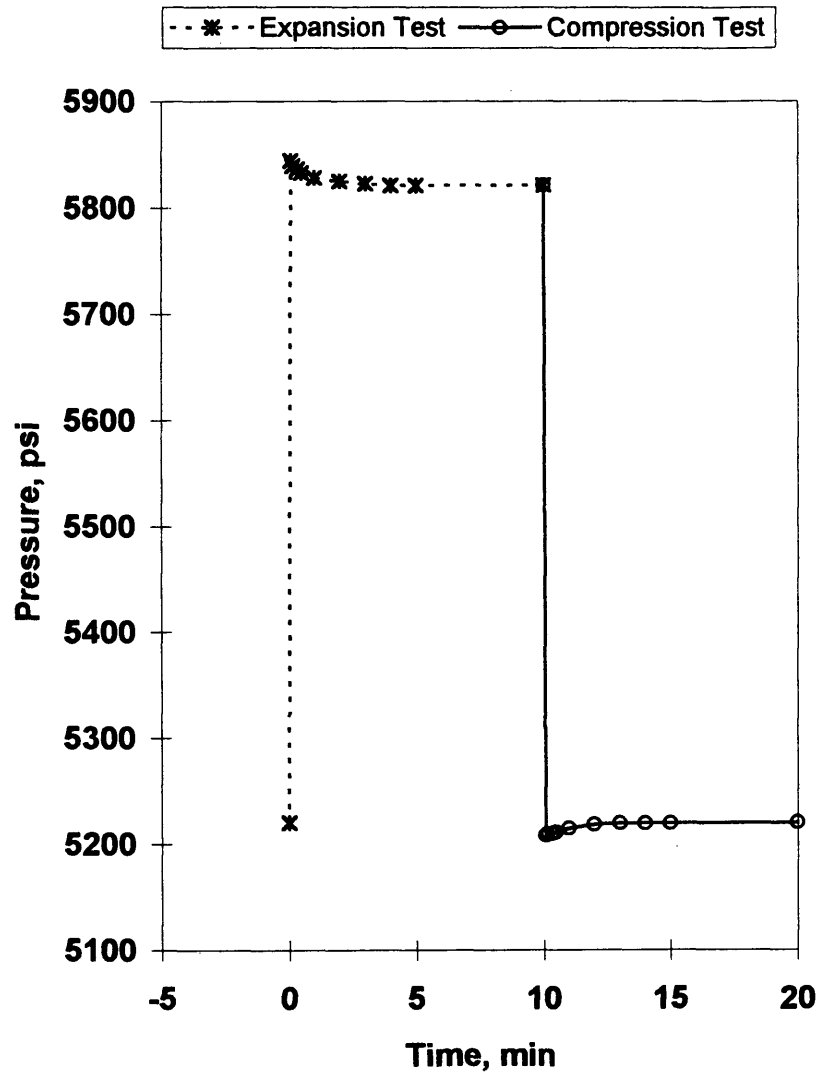


Figure 4.19 Pressure history for De-ionized water sample at 150°F (Run 2).

**Pressure History for Both Compression and
Expansion Test with De-ionized water sample at
200°F**

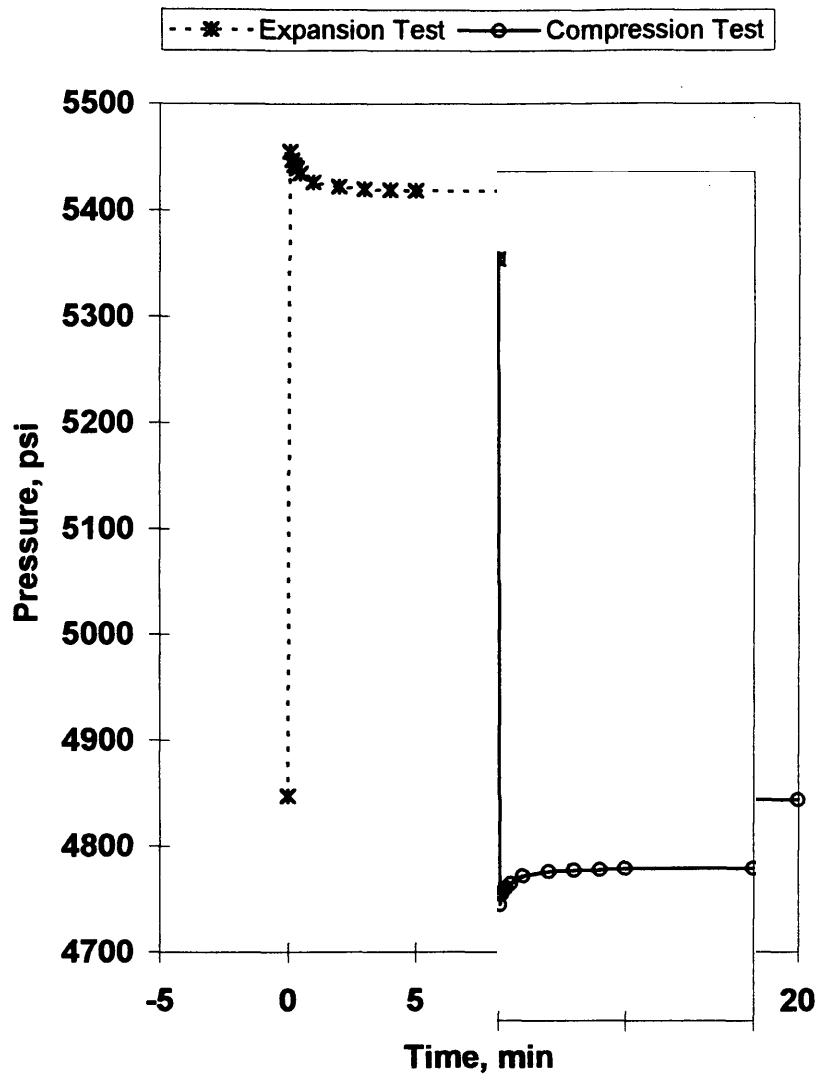


Figure 4.20 Pressure history for De-ionized water sample at 200°F (Run 1).

**Pressure History for Both Compression and
Expansion Test with De-ionized water sample at
200°F**

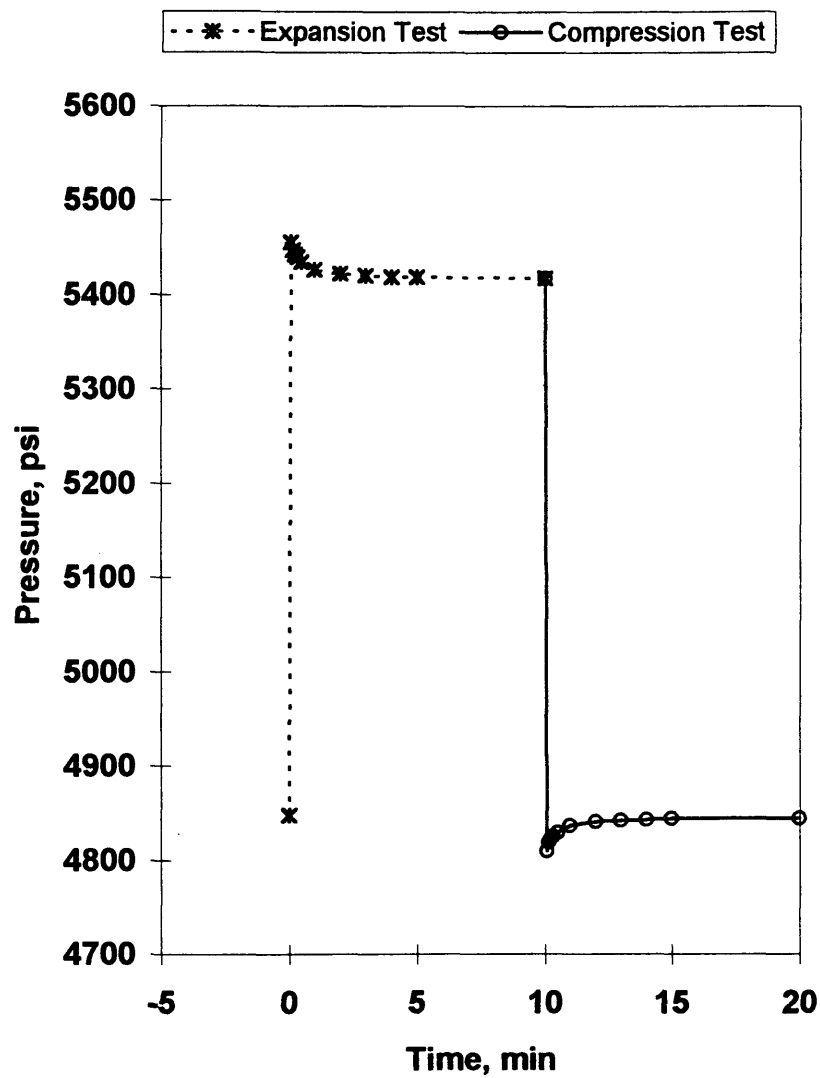


Figure 4.21 Pressure history for De-ionized water sample at 200°F (Run 2).

Heat Capacity Ratio for Water as a Function of Pressure

··· * ··· T=77 F -○- T=122 F -△- T=167 F -x- T=212 F - - - T=257 F -◆- T=302 F

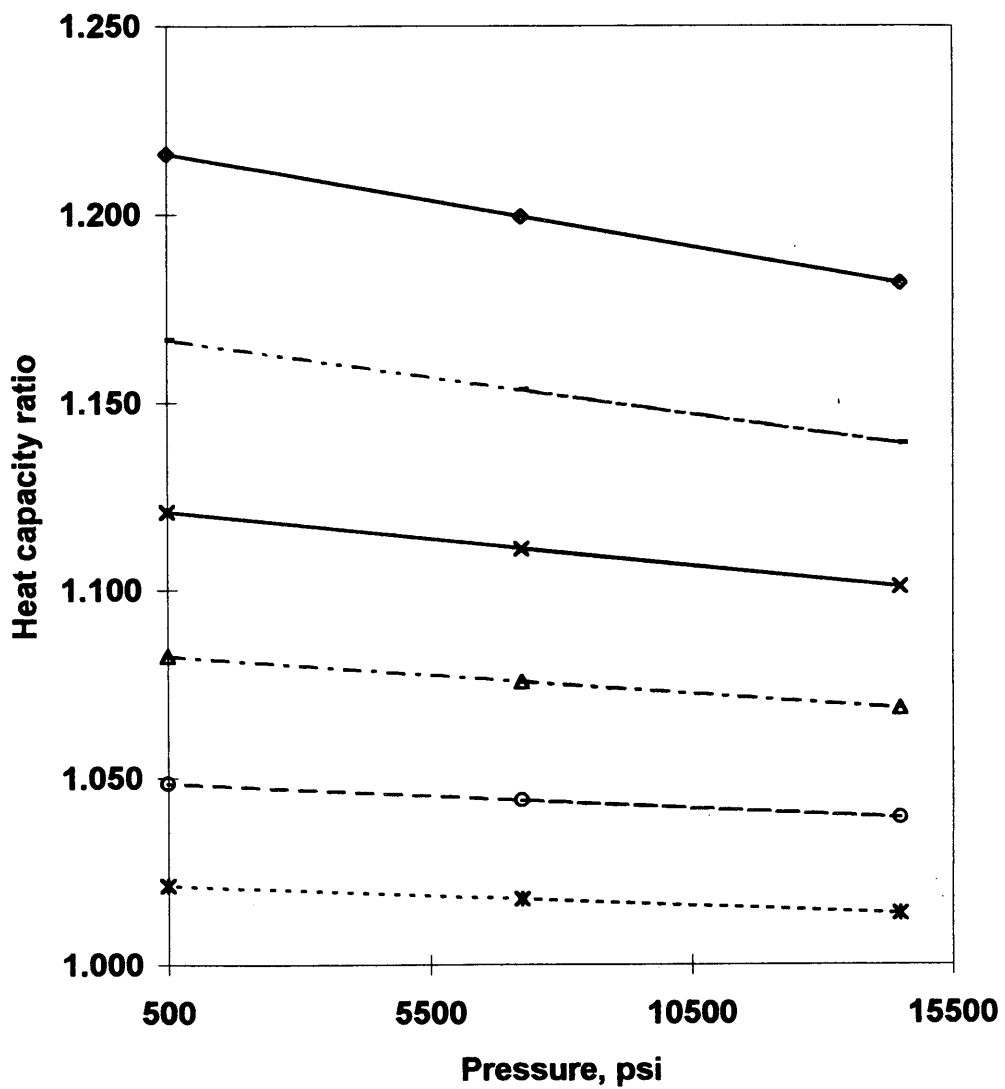


Figure 4.22 Water heat capacity ratio as a function of pressure (Helgeson and Kirkham, 1974).

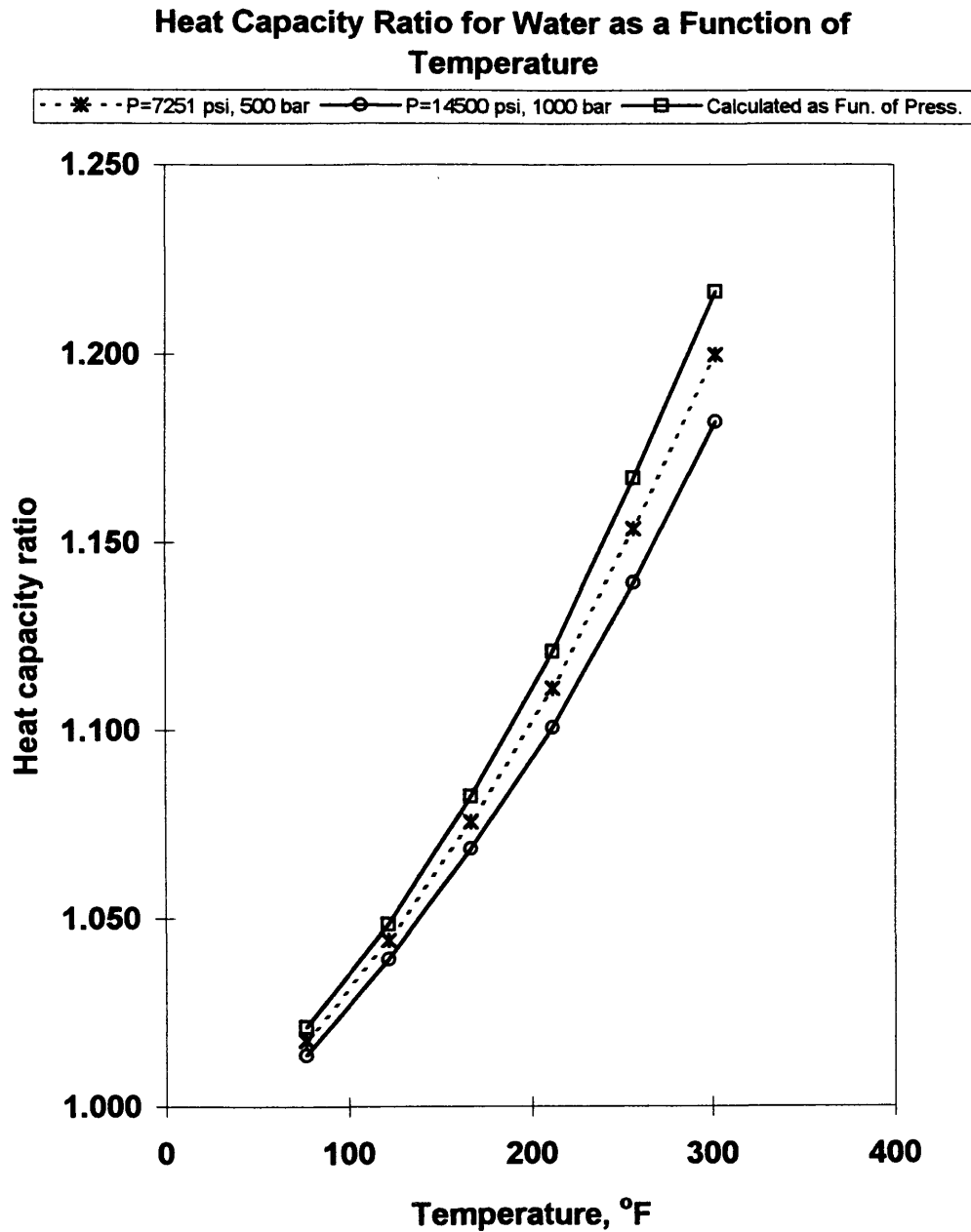


Figure 4.23 Water heat capacity ratio as a function of temperature (Helgeson and Kirkham, 1974).

Comparison of Measured and Literature values Sonic Velocity for De-ionized Water

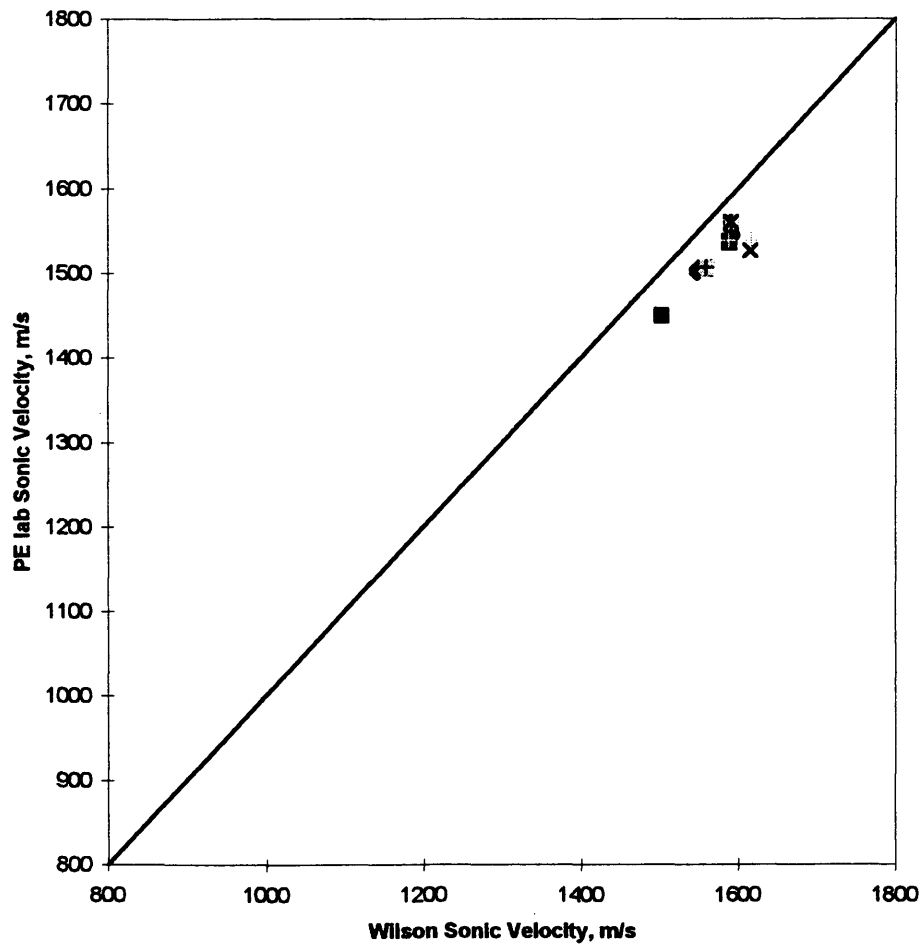
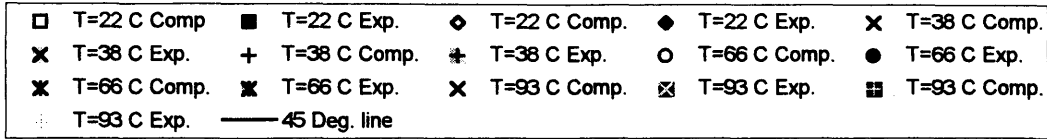


Figure 4.24 Sonic velocity values for De-ionized Water from Wilson(1959) and Petroleum laboratory measurement.

4.4 n-Pentane

Table 4.7 contains all of the measured isothermal compressibilities and heat capacity ratios for the n-pentane sample at different temperatures and pressures. As can be seen, the isothermal compressibilities from the PE Lab are within 5 to 15% of the literature values for most cases. The heat capacity ratios from the PE Lab are within 2% of the literature values for three experiments, and within about 20% for the others.

Table 4.8 includes the sonic velocity for n-pentane calculated from the literature and from the PE laboratory data using Eq. 2.12.

Figures 4.25 through 4.31 show the pressure histories for the n-pentane sample. Except for Fig. 4.28, all the figures show the exponential decline (the pressure raises to a peak value then it stabilizes) for the compression test, and the opposite shape for the expansion test. The compression history of Fig. 4.28 shows evidence of increased air bath temperature which was caused by response of the temperature control system to opening of the bath door. When the door was opened, the bath temperature decreased, then the control electronics responded by adding heat to raise the temperature. Figure 4.32 compares the sonic velocities from the available literature and laboratory measured values. All the sonic velocity measurements were lower than literature values, except for 40°C the sonic velocity

values were higher and that could be due to some error in the conducted experiments at that temperature.

Table 4.7 Measured and literature isothermal compressibilities and heat capacity ratios for n-pentane C₅H₁₂.

Temperature,		Test Method	Pressure,		Isothermal Compressibility, x 10 ⁶				Heat Capacity Ratio	
°C	°F		MPa	psi	PE lab		Vargaftik		PE lab	Vargaftik
					MPa ⁻¹	psi ⁻¹	MPa ⁻¹	psi ⁻¹		
20	68	Comp.	4.87	706	181	1.25	123	0.851	1.254	1.244
		(Fig 4.22) Exp.	4.88	707	184	1.27	127	0.877	1.240	1.259
40	104	Comp.	19.66	2851	165	1.14	187	1.29	1.215	1.201
		(Fig 4.23) Exp.	19.65	2850	164	1.13	191	1.32	1.185	1.201
40	104	Comp.	7.46	1081	203	1.40	244	1.68	1.225	1.220
		(Fig 4.24) Exp.	7.46	1081	202	1.39	248	1.71	1.207	1.223
60	140	Comp.	13.83	2006	193	1.33	194	1.34	1.086	1.321
		(Fig 4.25) Exp.	13.89	2015	218	1.50	199	1.37	1.233	1.319
60	140	Comp.	20.80	3016	184	1.27	167	1.15	1.190	1.365
		(Fig 4.26) Exp.	20.80	3016	186	1.28	170	1.17	1.191	1.355
80	176	Comp.	14.46	2097	255	1.76	264	1.82	1.228	1.445
		(Fig 4.27) Exp.	14.46	2097	257	1.77	270	1.86	1.224	1.430
80	176	Comp.	10.08	1461	276	1.90	291	2.01	1.187	1.373
		(Fig 4.28) Exp.	10.08	1462	284	1.96	312	2.15	1.210	1.366

Table 4.8 Calculated sonic velocity of n-pentane for both literature obtained and laboratory measured data.

Temperature, °C °F		Test Method	Pressure, MPa psi		Sonic velocity				
					PE lab		Vargaftik		
						m/s	ft/s	m/s	ft/s
20	68	Comp.	4.87	706	1052	2452	1264	4147	
		Exp.	4.88	707	1040	3412	1253	4111	
40	104	Comp.	19.66	2851	1085	3560	1008	3307	
		Exp.	19.65	2850	1077	3534	997	3271	
40	104	Comp.	7.46	1081	984	3229	891	2923	
		Exp.	7.46	1081	980	3215	884	2900	
60	140	Comp.	13.83	2006	950	3117	1037	3402	
		Exp.	13.89	2015	954	3130	1026	3366	
60	140	Comp.	20.80	3016	1019	3343	1139	3737	
		Exp.	20.80	3016	1015	3330	1125	3691	
80	176	Comp.	14.46	2097	879	2884	932	3058	
		Exp.	14.46	2097	875	2871	917	3009	
80	176	Comp.	10.08	1461	832	2730	864	2835	
		Exp.	10.08	1462	827	2713	833	2733	

**Pressure History for Both Compression and
Expansion Test with Pentane at 68°F**

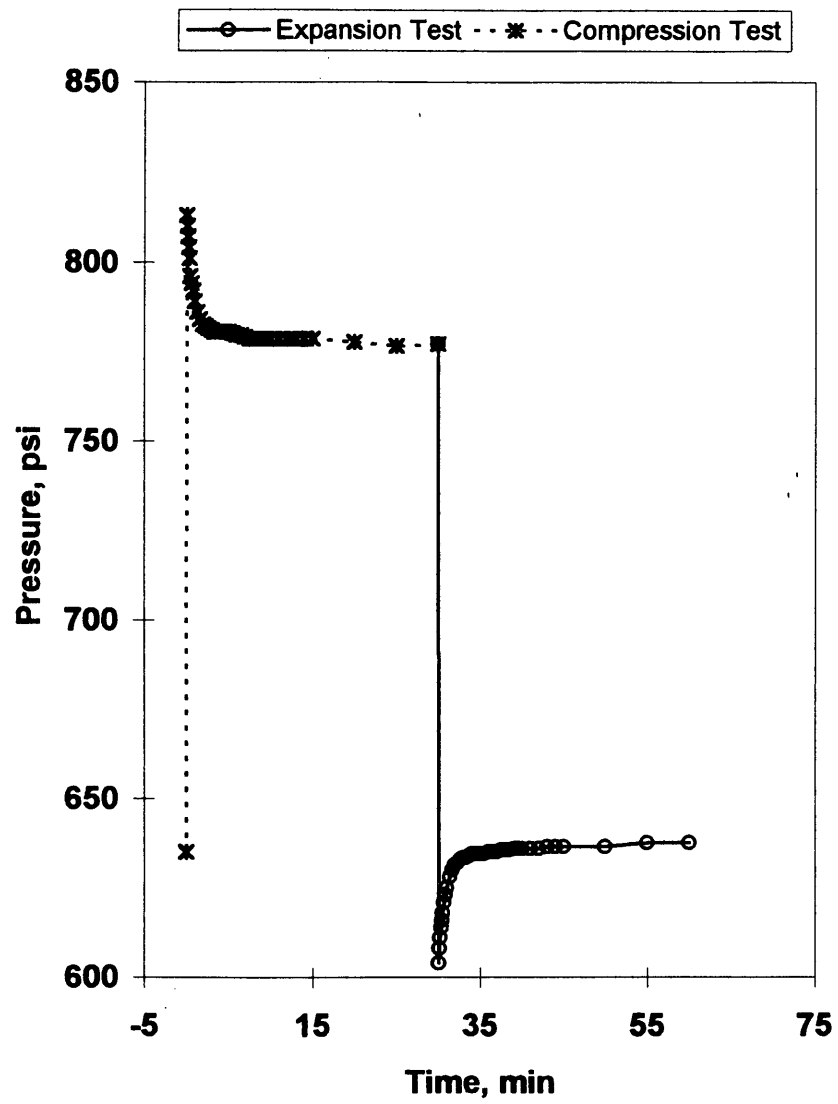


Figure 4.25 Pressure history for Pentane sample at 68°F.

**Pressure History for Both Compression and
Expansion Test with Pentane at 104°F**

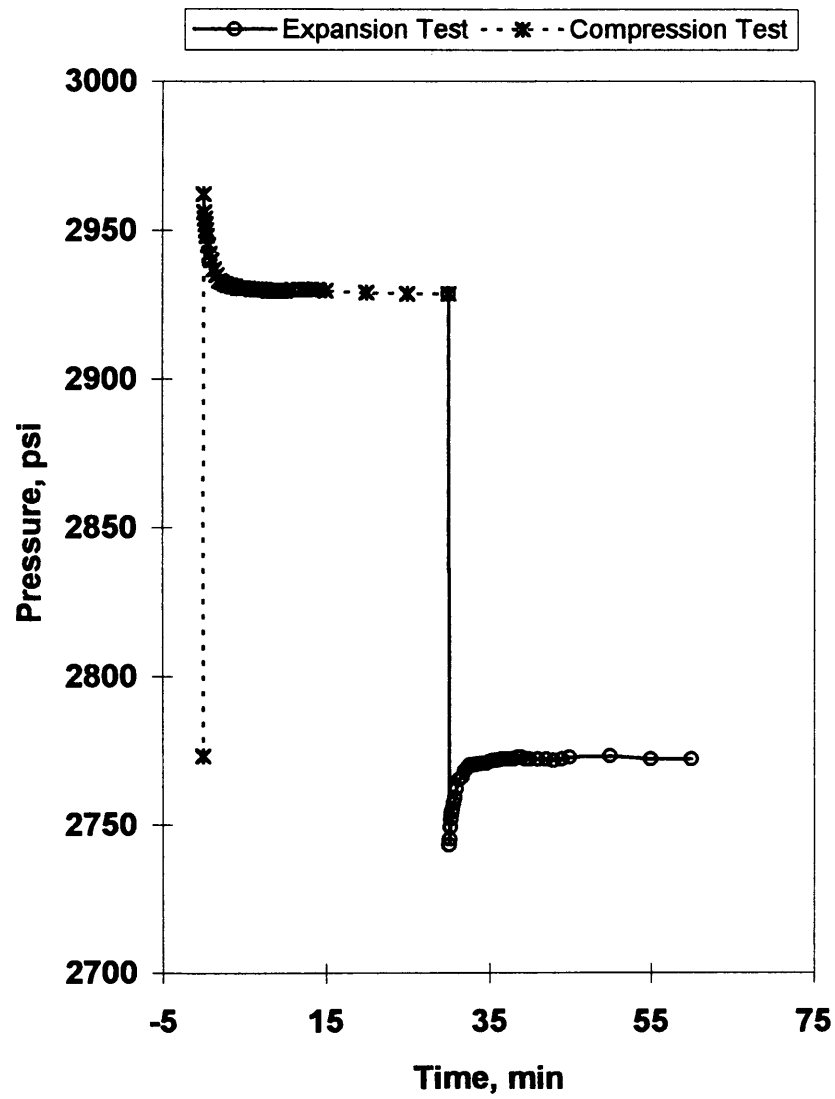


Figure 4.26 Pressure history for Pentane sample at 104°F (Run 1).

**Pressure History for Both Compression and
Expansion Test with Pentane at 104°F**

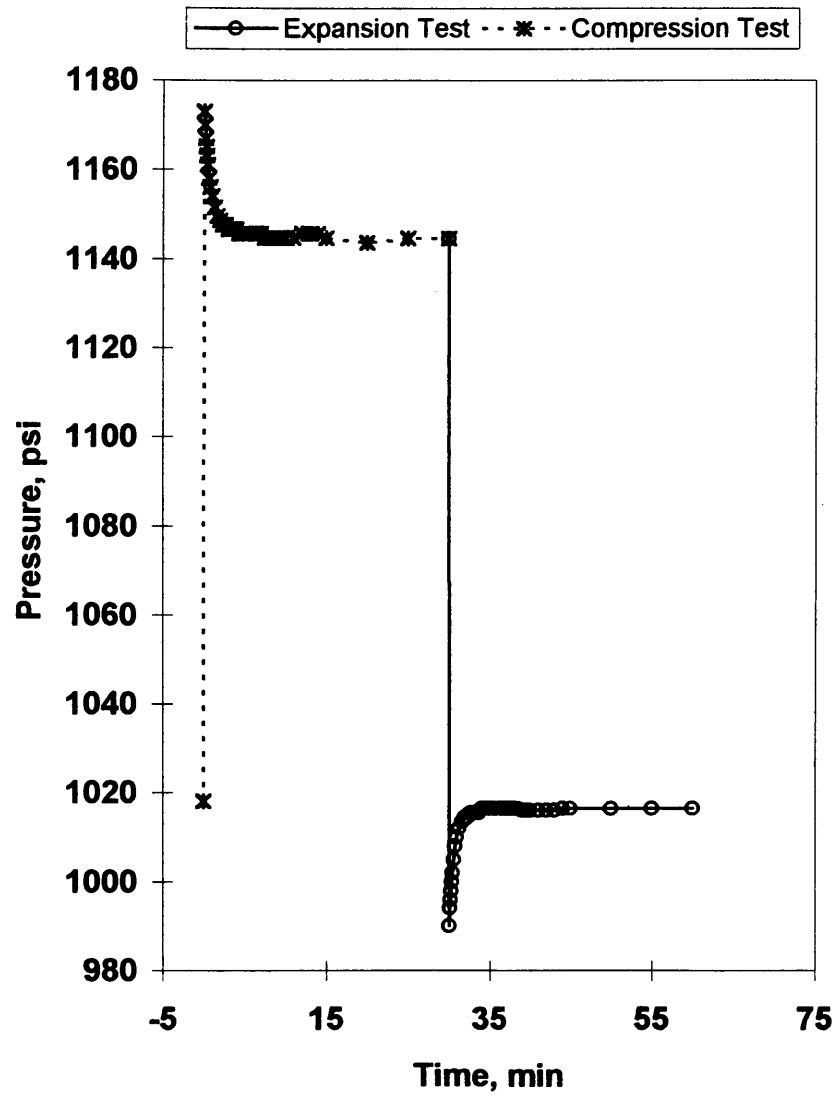


Figure 4.27 Pressure history for Pentane sample at 104°F (Run 2).

**Pressure History for Both Compression and
Expansion Test with Pentane at 140°F**

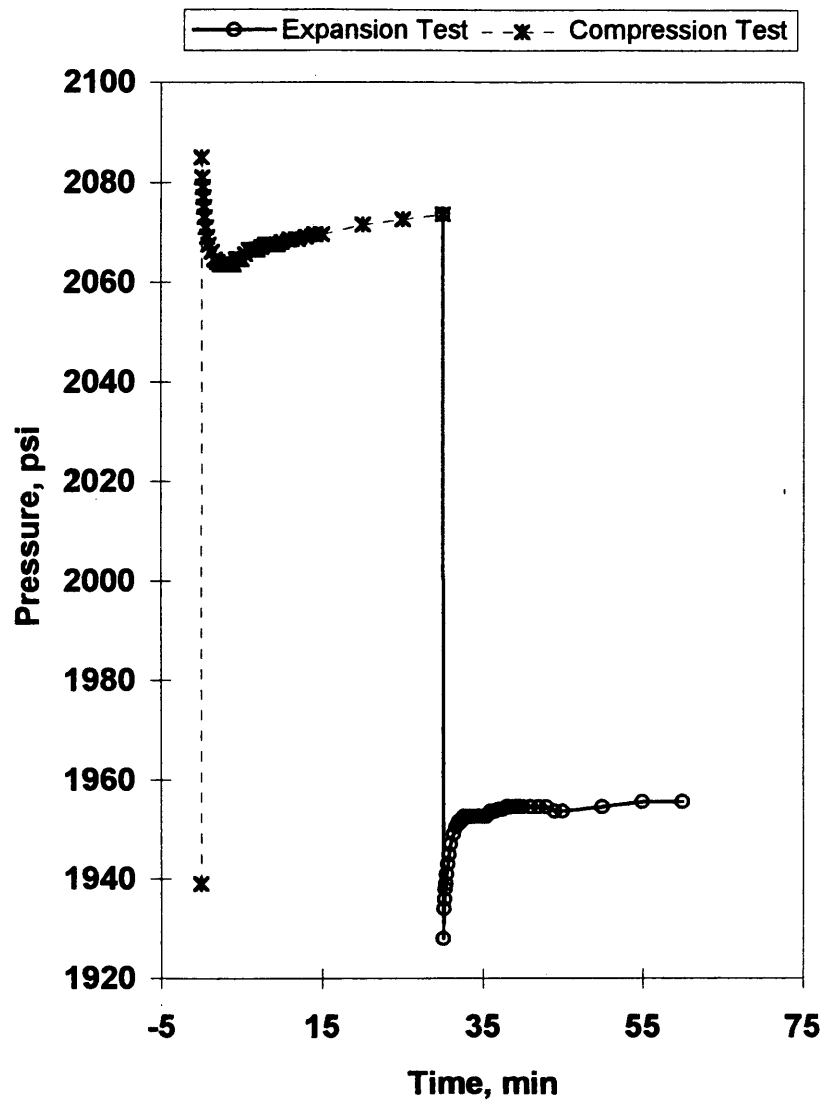


Figure 4.28 Pressure history for Pentane sample at 140°F (run 1).

**Pressure History for Both Compression and
Expansion Test with Pentane at 140°F**

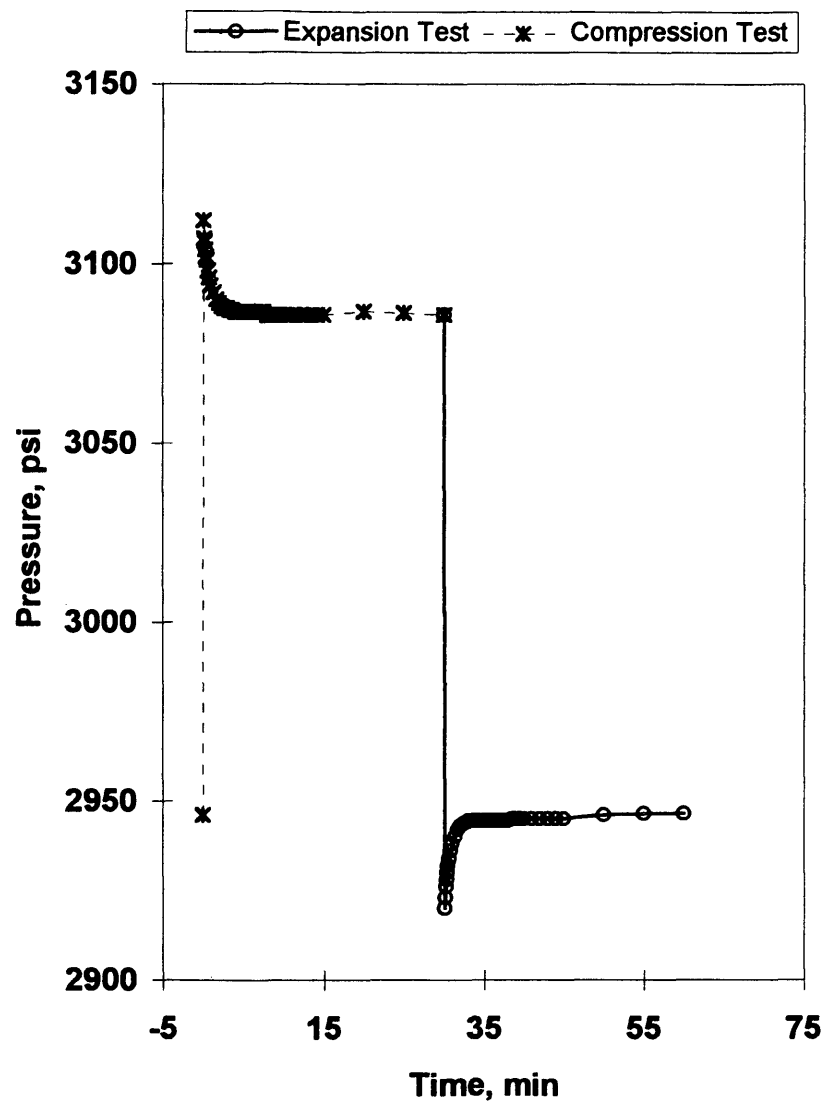


Figure 4.29 Pressure history for Pentane sample at 140°F (run 2).

**Pressure History for Both Compression and
Expansion Test with Pentane at 176°F**

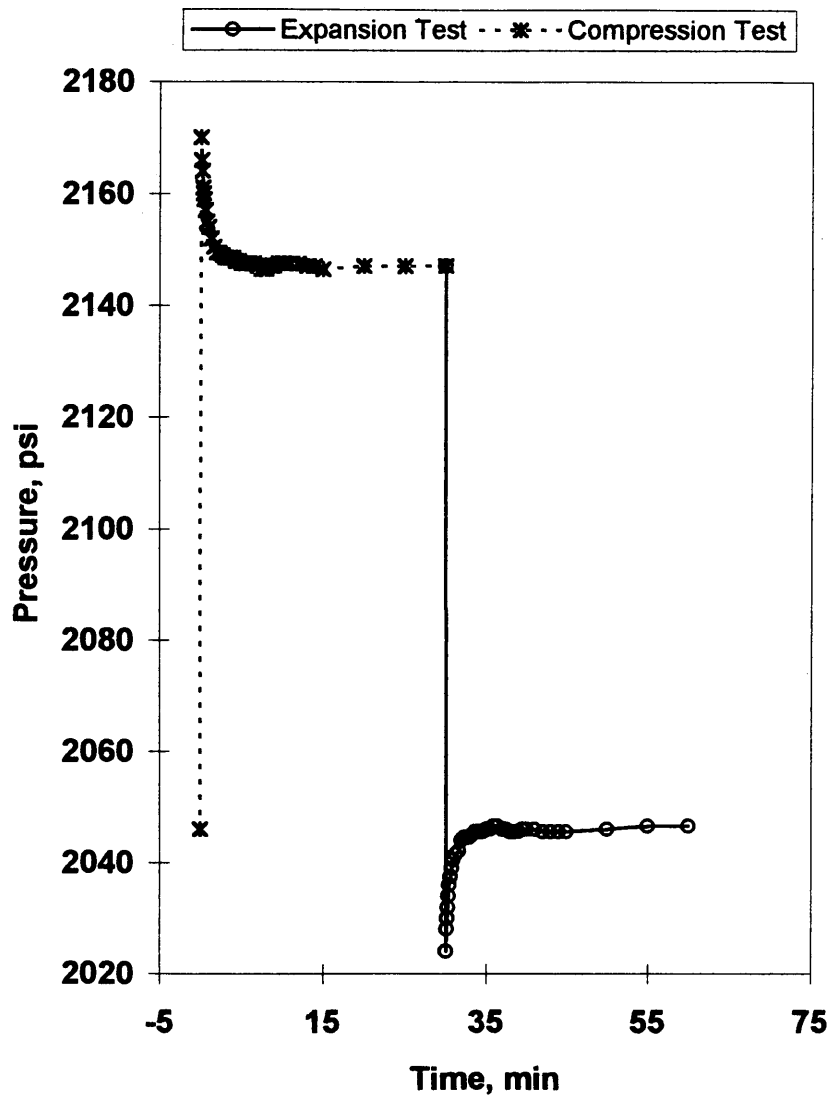


Figure 4.30 Pressure history for Pentane sample at 176°F (run 1).

**Pressure History for Both Compression and
Expansion Test with Pentane at 176°F**

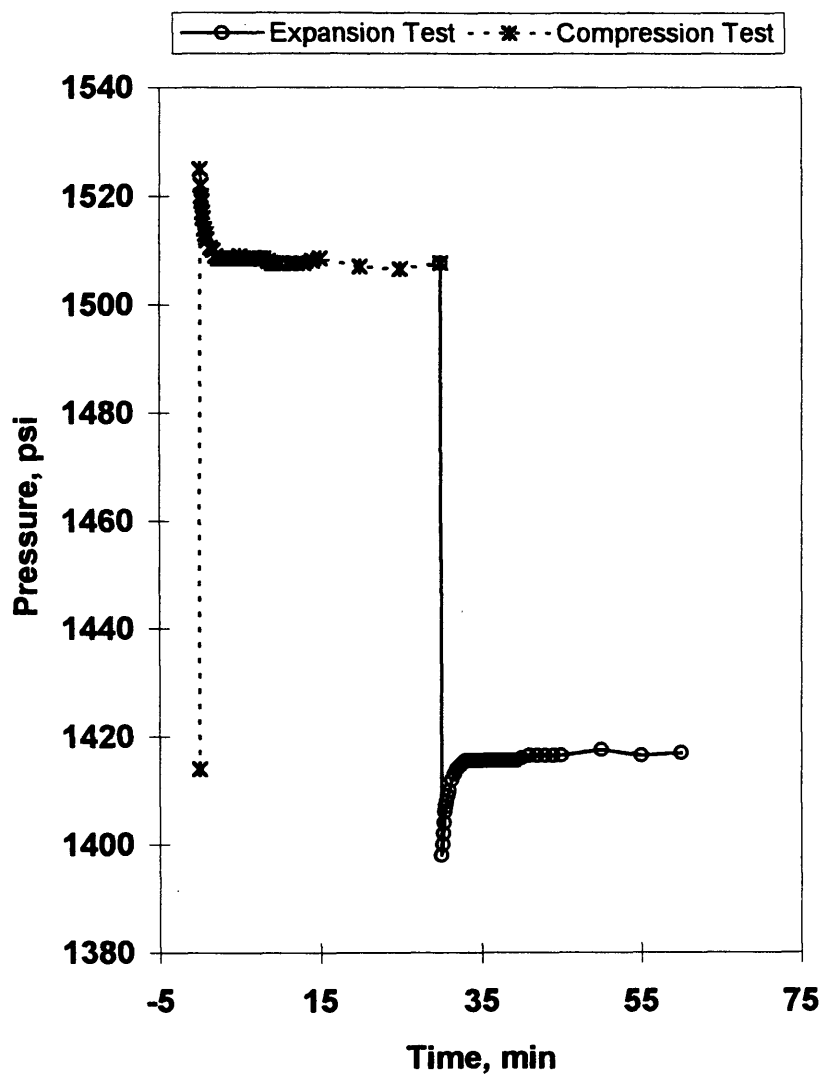


Figure 4.31 Pressure history for Pentane sample at 176°F (run 2).

Comparison of Measured and Literature Values Sonic Velocity for n- Pentane

□ T=20 C Comp.	■ T=20 C Exp.	◇ T=40 C Comp.	◆ T=40 C Exp.	△ T=40 C Comp.
▲ T=40 C Exp.	○ T=60 C Comp.	● T=60 C Exp.	× T=60 C Comp.	✕ T=60 C Exp.
⊠ T=80 C Comp.	⊗ T=80 C Exp.	⊕ T=80 C Comp.	⊖ T=80 C Exp.	— 45 Deg. line

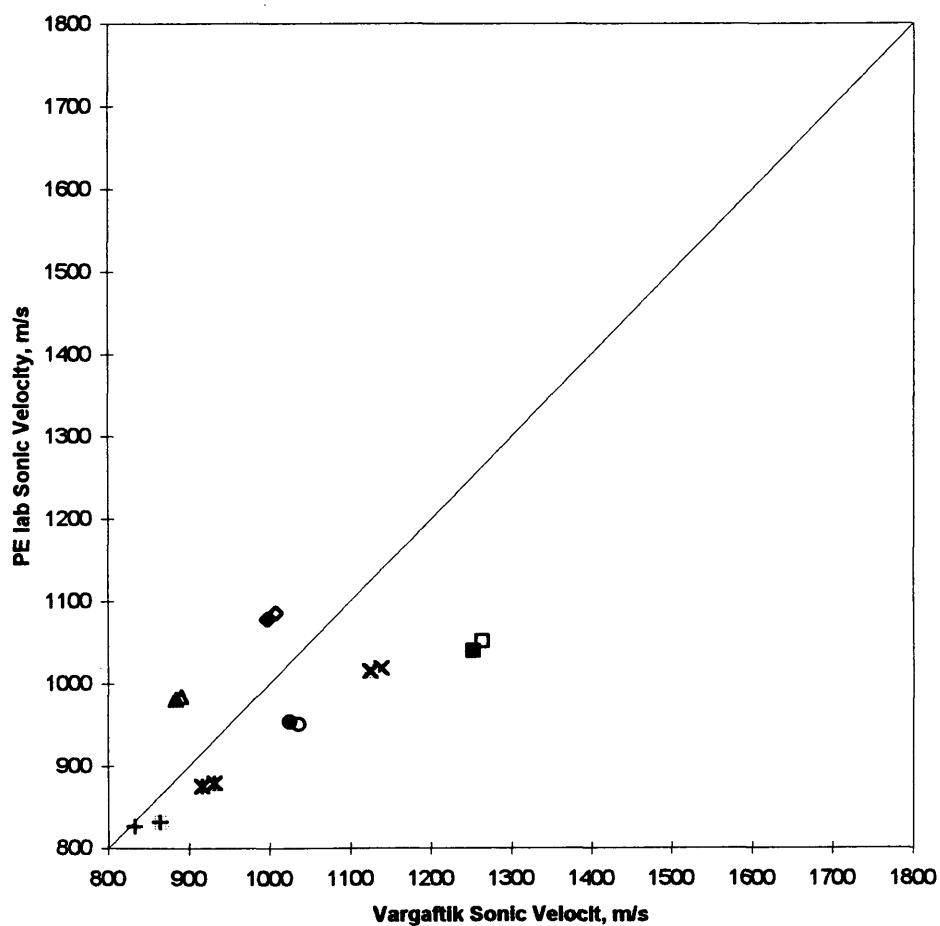


Figure 4.32 Sonic velocity values for n-Pentane from Vargaftik(1983) and Petroleum laboratory measurement.

CHAPTER FIVE

CONCLUSIONS AND RECOMMENDATIONS

5.1 Conclusions

As a result of this research, the following conclusions are proposed:

1. Fluid densities were measured at standard conditions. The results were within 2% of the literature values.

2. An apparatus was assembled for measuring isothermal compressibility of fluids. With this apparatus, it is generally possible to measure isothermal compressibilities within 10% of literature values.

3. While testing the apparatus, it was noticed that instantaneously after decreasing the cell volume, the pressure rose rapidly and then slowly decreased to a stable reading. The ratio of the instantaneous pressure rise to the stabilized pressure decline is the heat capacity ratio of the fluid in the apparatus. Heat capacity ratios measured with the apparatus are generally within 10% of literature values.

4. Using thermodynamically derived expressions, sonic velocities can be estimated with satisfactory accuracy for single-phase fluids with densities, isothermal compressibilities, and heat capacity ratios measured with the apparatus assembled for this research. The square-root dependence of sonic velocity on density, isothermal compressibility, and heat capacity ratio, as shown in Eq. 2.12, minimizes the propagation of errors.

5. Laboratory measured sonic velocities turned to be smaller than the literature obtained values for the tested samples and this could be explained and referred to as an error in estimating the adiabatic compressibility rather than the isothermal compressibility, and it can also be affected by the room temperature density measurements.

6. Sonic velocities for n-decane, as estimated with data from the apparatus, are within 1 to 16 % of literature and other measured values. The differences are largely due to inconsistencies between the measured and the literature values for isothermal compressibility. It is hoped that with more experience, the measurements of compressibility will become more accurate. Heat capacity ratios of n-decane were within 12% of literature values.

7. Sonic velocities for de-ionized water estimated with Eq. 2.12 from this research were within 10% of estimates with Eq. 2.12 based on literature data.

Measured heat capacity ratios were within 5% of literature values. Measured isothermal compressibilities were within 20% of literature values.

8. Sonic velocities for the Burly oil sample, as estimated with Eq. 2.12, were within 6% of the values reported by Prof. Batzle in the Geophysics Department.

9. For n-pentane sample, the sonic velocities estimated with Eq. 2.12 from measurements of density, isothermal compressibility, and heat capacity ratio were within 20% of literature values estimated with Eq. 2.12. Some of the estimates were within 1%.

5.2 Recommendations

The following recommendations are suggested for future work:

1. An equation of state (EOS) such as the Peng-Robinson EOS should be used to estimate the isothermal compressibilities and heat capacity ratios of fluids. Although there might be some discrepancy between the lab measurements and the estimates obtained from the EOS, it is believed that the EOS may yield satisfactory estimates of seismic velocities because of cancellation of errors in the various components of the velocity expression. Methods to improve the EOS estimates should be explored.

2. Data acquisition with a computer interface is essential for improving the quality of the pressure histories measured with the apparatus of Figure 3.1. For the current research, pressures were manually recorded. Although manual recording was sufficient to demonstrate the approach, rapid data acquisition that would be possible with a computer is needed to improve the estimates of sonic velocities. In a step toward automation, the Micro-pump in the apparatus of Figure 3.1 has already been upgraded with an air operated valve. This new valve provides similar volume change to the old valve, but with much faster actuation. Faster actuation should produce better peak pressure readings, which in turn will lead to better heat capacity ratio estimation. It is anticipated that the valve could be actuated by a signal from a computer control system.

3. Density measurement should be integrated with the apparatus so that the complete set of data (density, isothermal compressibility, and heat capacity ratio) needed for estimating sonic velocity can be obtained. A vibrating tube densitometer is available for this application. Work has already begun to combine this densitometer with the apparatus.

4. Further effort to demonstrate reliability of all measurements should be an essential part of the future of this program for estimating sonic velocities. Some differences between measured and literature values of isothermal

compressibility of water were noted. These differences should be investigated to determine if they represent a systematic error in the apparatus or if they are a valuable correction to the literature. It is hoped that automated data acquisition will improve the quality of the data from the apparatus.

5. Correlations for estimating isothermal heat capacities of a wide variety of crude oils should be compared with measurements. Also, correlations for estimating heat capacity ratios for crude oils should be developed.

REFERENCES

- Andsager, R. L., and Knapp, R. M. 1967. Acoustic Determination of Liquid Levels in Gas wells. JPT. p. 601-605.
- Batzle, M. L. 1996. Fluid Properties Consortium. Annual Report. Colorado School of Mines, Golden, CO.
- Bird, R. B., Stewart, W. E., and Lightfoot, E. N. 1960. Transport Phenomena. John Wiley & Sons, New York p. 352-360
- Castanga, J. P., Batzle, M. L., and Kan, T. K. 1993. Rock Physics-The link between Rock Properties and AVO Response. SEG, Investigation in Geophysics No. 8, Tulsa, OK, p. 135-171.
- Fowler, R. G., and Meyer, D. I. 1958. Physics for Engineers and Scientists . Allyn and Bacon, Inc., p. 409-411.
- Helgeson, Harold, C., and Kirkham, David, H. 1974. Theoretical prediction of the Thermodynamic Behavior of Aqueous Electrolytes at High Pressure and temperatures: I. Summary of the Thermodynamic/Electrostatic Properties of the solvent. American Journal of Science. p. 1098-1159.
- Hougen, O. A., Watson, K. M., and Ragatz, R. A. 1974. Chemical Process Principles . Part II, Thermodynamic, John Wiley & Sons, Inc., New York p. 541.
- Kearey, Philip & Brooks, Michael. 1991. An Introduction to Geophysical Exploration . Second Edition, Black Well Scientific Publications, Oxford, London p. 23-26.
- Keiffer, S. W. 1977. Sound speed in Liquid-Gas Mixtures: Water-Air and Water-Steam. Journal of Geophysical Research, 82, 20.

- Kreith, F. 1973. Principles of Heat Transfer. Third Edition. Intext Educational Publishers, New York p. 634.
- Kyle, B. G. 1992. Chemical and Process Thermodynamics. Second Edition, Prentice Hall, Englewood Cliffs, New Jersey, p. 23, 24.
- Macias, L. C., and Ramey, H. J. 1986. Multiphase, Multicomponent compressibility in petroleum reservoir Engineering. SPE paper 15538 presented in the 61st Annual meeting in New Orleans L.A., October 5-8.
- McCain, W. D. Jr. 1990. The Properties of Petroleum Fluids . Second Edition, Penn Well Books, Tulsa, Oklahoma p. 231.
- Smith, J. M., Nan Ness, H. C. 1975. Introduction to Chemical Engineering Thermodynamics . Third Edition, McGRAW-HILL International Book Company, international Student Edition, p. 48-52.
- Thomas, L. K. Aug. 1968. A review of the Acoustic Determination of Liquid Levels in Gas Wells. JPT p. 784-785.
- Vargaftik, N. B. 1983. Handbook of Physical Properties of Liquid and Gases. Second Edition. Hemisphere Publishing Corporation, New York. p. 280-282.
- _____. 1983. Handbook of Physical Properties of Liquid and Gases. Second Edition. Hemisphere Publishing Corporation, New York. p. 255-259.
- Walas, S. M. 1985. Phase Equilibria in Chemical Engineering. Butterworth Publishers, Boston. p. 501.
- Wang, Z. J., Nur, A. M., Batzle, M. L. 1988. Acoustic Velocities in Petroleum Oils . SPE paper No. 18163, Proceeding 63, p. 571-584.
- Wang, Z. J., Batzle, M. L., and Nur, A. M., 1990. The Role of Fluid Properties on Seismic Interpretation . Canadian Journal of Exploration and Geophysics, 26, p. 104-112.

Weast, R. C. 1971. CRC Handbook of Chemistry and Physics. 52nd Edition. The Chemical Ruffer Company, Cleveland, Ohio. p. F-11.

Wilson, W. D. 1959. Speed of Sound in Distilled Water as a Function of Temperature and Pressure. The Journal of the Acoustical Society of America. Volume 31, Number 8, p.1067-1072.

APPENDICES

Appendix A-1

Isothermal compressibility values from Vargaftik (1983) for n-decane and the equivalent conversion to field units are compiled here. To convert pressure from atm to psi, Vargaftik's values were multiplied by 14.69; for example,

$$20 \text{ atm} * 14.69 = 294 \text{ psi}$$

To convert isothermal compressibility from $\frac{\text{cm}^2}{\text{kg}}$ to psi^{-1} , Vargaftik's values were multiplied by $0.07045 * 10^{-7}$; for example,

$$1652 \frac{\text{cm}^2}{\text{kg}} * 0.07045 * 10^{-7} = 1.16\text{E}^{-5} \text{ psi}^{-1}$$

T = 40°C = 104°F

Pressure, atm	$\beta 10^7, \text{cm}^2/\text{kg}$	Pressure, psi	c, psi^{-1}
20	1652	294	1.16E-5
40	1490	588	1.05E-5
60	1365	881	9.62E-6
80	1264	1175	8.91E-6
100	1160	1469	8.17E-6
120	1077	1763	7.59E-6
140	997	2057	7.02E-6
160	945	2350	6.66E-6
180	870	2644	6.13E-6
200	822	2938	5.80E-6

T = 60°C = 140°F

Pressure, atm	$\beta \cdot 10^7, \text{cm}^2/\text{kg}$	Pressure, psi	c, psi^{-1}
20	1994	294	1.41E-5
40	1800	588	1.27E-5
60	1615	881	1.13E-5
80	1474	1175	1.04E-5
100	1339	1469	9.43E-6
120	1211	1763	8.53E-6
140	1118	2057	7.88E-6
160	1029	2350	7.25E-6
180	944	2644	6.65E-6
200	889	2938	6.26E-6

T = 80°C = 176°F

Pressure, atm	$\beta \cdot 10^7, \text{cm}^2/\text{kg}$	Pressure, psi	c, psi^{-1}
20	2454	294	1.73E-5
40	2136	588	1.51E-5
60	1921	881	1.35E-5
80	1694	1175	1.19E-5
100	1524	1469	1.07E-5
120	1378	1763	9.71E-6
140	1238	2057	8.72E-6
160	1138	2350	8.02E-6
180	1029	2644	7.25E-6
200	950	2938	6.69E-6

Appendix A-2

Isothermal compressibility values from Vargaftik (1983) for n-pentane and the equivalent conversion in field units are compiled here. To convert pressure from atm to psi, Vargaftik's values were multiplied by 14.696; for example,

$$20 \text{ atm} * 14.69 = 294 \text{ psi}$$

To convert isothermal compressibility from atm^{-1} to psi^{-1} , Vargaftik's values were divided by 14.696, for example,

$$\frac{401 * 10^{-6}}{14.696} = 2.73\text{E}^{-5} \text{ psi}^{-1}$$

$$\mathbf{T = 40^{\circ}\text{C} = 104^{\circ}\text{F}}$$

Pressure, atm	$\beta 10^6, \text{ atm}^{-1}$	Pressure, psi	c, psi^{-1}
20	248	294	1.69E-5
40	238	588	1.62E-5
60	229	882	1.56E-5
80	218	1175	1.48E-5
100	210	1470	1.43E-5
150	190	2204	1.29E-5
200	174	2939	1.18E-5

$$T = 60^{\circ}\text{C} = 140^{\circ}\text{F}$$

Pressure, atm	$\beta \cdot 10^6, \text{atm}^{-1}$	Pressure, psi	c, psi^{-1}
20	313	294	2.13E-5
40	296	588	2.01E-5
60	280	882	1.91E-5
80	266	1175	1.81E-5
100	253	1470	1.72E-5
150	224	2204	1.52E-5
200	199	2939	1.35E-5

$$T = 80^{\circ}\text{C} = 176^{\circ}\text{F}$$

Pressure, atm	$\beta \cdot 10^6, \text{atm}^{-1}$	Pressure, psi	c, psi^{-1}
20	401	294	2.73E-5
40	375	588	2.55E-5
60	350	882	2.38E-5
80	327	1175	2.23E-5
100	307	1470	2.09E-5
150	265	2204	1.80E-5
200	229	2939	1.56E-5